Applied Energy 308 (2022) 118370

Contents lists available at ScienceDirect

Applied Energy

journal homepage: www.elsevier.com/locate/apenergy

Case study on optimal design and operation of detached house energy system: Solar, battery, and ground source heat pump

Ellen Nordgård-Hansen [a,*], Nand Kishor [b,c], Kirsti Midttømme [d], Vetle Kjær Risinggård [e], Jan Kocbach [f]

[a] NORCE Norwegian Research Centre, Jon Lilletuns vei 9 H, 3. et, NO-4879 Grimstad, Norway
[b] Østfold University College, Postboks 700, NO-1757 Halden, Norway
[c] Motilal Nehru National Institute of Technology Allahabad, Prayagraj 211004, India
[d] NORCE Norwegian Research Centre, Postboks 22 Nygårdstangen, NO-5838 Bergen, Norway
[e] NORCE Norwegian Research Centre, Universitetsveien 19, NO-4630 Kristiansand, Norway
[f] NORCE Norwegian Research Centre, Postboks 22 Nygårdstangen, NO-5838 Bergen, Norway

HIGHLIGHTS

- Energy policies can be evaluated by considering optimal energy system operation.
- Feed-in tariffs encourage to not use boreholes for seasonal energy storage.
- Ground-source heat pump systems are more profitable for capacity tariffs.

ARTICLE INFO

Keywords:
Borehole thermal energy storage (BTES)
Mixed integer linear programming
Demand response management
Residential buildings
Energy system sustainability
Energy policy

ABSTRACT

Government policy impacts the level of sustainability for which houseowners design and operate their energy system. Consequently, there is a need to consider the sustainability level resulting from different policies, assuming optimal design and operation. The present work focuses on detached residential houses, where the energy system consists of photovoltaic systems for energy generation and batteries and optional ground-source heat pump systems for energy storage. A mixed-integer linear programming model is presented, which takes policies and other constraints into account when optimizing system size and operation. The results allow overall sustainability validation through parameters like self-sufficiency and self-sustainability, as well as a detailed drill-down of the optimal operation. From the analysis, two modes of ground-source heat pump usage are seen. With a feed-in tariff present, its main use is as an energy source, while without this tariff the optimal use is for seasonal energy storage. It is also found that ground-source heat pump systems contribute to increased sustainability, but they may not be economically beneficial for single-family homes having low or medium heating requirements. Demands for heating and cooling change with time and place, as do available area for photovoltaic energy generation and externally available energy sources. Therefore, a detailed analysis of the kind presented here is recommended before new energy policies are implemented. For each specific house or project, this kind of analysis will also be useful to evaluate the sensitivity of an energy system's performance towards changing policies.

* Corresponding author.
E-mail addresses: enor@norceresearch.no (E. Nordgård-Hansen), nand.kishor@hiof.no (N. Kishor), kimi@norceresearch.no (K. Midttømme), veri@norceresearch.no (V.K. Risinggård), jako@norceresearch.no (J. Kocbach).

https://doi.org/10.1016/j.apenergy.2021.118370
Received 22 June 2021; Received in revised form 14 November 2021; Accepted 6 December 2021
Available online 18 December 2021

Glossary and symbols

Abbreviation

BHE	Borehole heat exchanger
BTES	Borehole thermal energy storage
CES	Community energy storage
COP	Coefficient of performance
EAC	Equivalent annual cost
GHI	Global horizontal irradiation
GSHP	Ground-source heat pump
MILP	Mixed-integer linear programming
PV	Photovoltaic
SC	Self-consumption
SOC	State of charge
SS	Self-sufficiency
UTES	Underground thermal energy storage
ZEB	Zero-emission buildings

Symbol

COP_c	Carnot coefficient of performance [–]
COP_i	Coefficient of performance for GSHP number i [–]
I	Investment cost [USD]
L	Total length of all boreholes [m]
M	A big number [–]
N	Final time step number [–]
$\dot{Q}$	Heat extraction rate [J/(s m)]
Q_{electric}	Electric heat supplied to the heat pump [J/s]
$Q_{\text{useful heat}}$	Useful heat supplied to the building [J/s]
SOC	State of charge [J]
T_b	Borehole wall temperature [K]
$T_{f,\in}$	Temperature of fluid entering borehole [K]
$T_{f,out}$	Temperature of fluid leaving borehole [K]
$\widehat{T}_{f,out}$	Estimate for temperature of fluid leaving borehole [K]
T_g	Undisturbed ground temperature [K]
T_h	High temperature [K]
ΔT_{b-f}	Temperature difference between borehole wall and fluid leaving borehole [K]
ΔT_{max}	Maximum allowed temperature change of borehole wall [K]
av_{GSHP_i}	Power available from GSHP number i [W]
av_{PV}	Power available from PV panels [W]
av_{util}	Power available from utility [W]
c_b	Total battery-related cost [USD]
$c^{b,e}_{b\to el}$	Battery energy cost for energy flowing from battery to el load [USD]
$c^{b,e}_{b\to hw}$	Battery energy cost for energy flowing from battery to hot water load [USD]
$c^{b,t}$	Battery time cost [USD]
c_{GSHP_i}	Total cost related to GSHP number i [USD]
$c^{GSHP_i,e}_{GSHP_i\to hw}$	Energy cost for GSHP number i for energy from GSHP to hot water load [USD]
$c^{GSHP_i,t}$	Time cost for GSHP number i [USD]
c_{PV}	Total PV-related cost [USD]
$c^{PV,e}_{PV\to b}$	PV energy cost for energy flowing from PV to battery [USD]
$c^{PV,e}_{PV\to el}$	PV energy cost for energy flowing from PV to el load [USD]
$c^{PV,e}_{PV\to hw}$	PV energy cost for energy flowing from PV to hot water load [USD]
$c^{PV,t}$	PV time cost [USD]
$c^{PV,e}_{PV\to util}$	PV energy cost for energy flowing from PV to utility [USD]
c_{tot}	Total cost [USD]
c_{util}	Total utility-related cost [USD]
$c^{util,c}$	Utility capacity cost [USD]
$c^{util,e}_{util\to el}$	Utility energy cost for energy flowing from utility to el load [USD]
$c^{util,e}_{util\to hw}$	Utility energy cost for energy flowing from utility to hot water load [USD]
$c^{util,e}_{util\to GSHP_i}$	Utility energy cost for energy flowing from utility to GSHP number i [USD]
$c^{util,p}_{PV\to util}$	Utility profit for energy flowing from PV to utility [USD]
$c^{util,t}$	Utility time cost [USD]
dt	Time step size [s]
ex_i	Existence of GSHP number i [–]
$f_{b\to el}$	Power flow from battery to electric load [W]
$f_{b\to hw}$	Power flow from battery to hot water load [W]
$f_{\text{GSHP}_i\to hw}$	Power flow from GSHP number i to hot water load [W]
$f_{PV\to b}$	Power flow from PV panels to battery [W]
$f_{PV\to el}$	Power flow from PV panels to electric load [W]
$f_{PV\to hw}$	Power flow from PV panels to hot water load [W]
$f_{PV\to util}$	Power flow from PV panels to utility [W]
$f_{util\to el}$	Power flow from utility to electric load [W]
$f_{PV\to \text{GSHP}_i}$	Power flow from PV panels to GSHP number i [W]
$f_{util\to \text{GSHP}_i}$	Power flow from utility to GSHP number i [W]
$f_{util\to hw}$	Power flow from utility to hot water load [W]
g_{func}	Borehole g-function [–]
i	GSHP number [–]
k_s	Thermal conductivity of the soil [W/(m K)]
l_{el}	Electric load [W]
l_{hw}	Hot water load [W]
m	Number of years [–]
n	Time step number [–]
r	Interest rate [–]
η_{bc}	Efficiency of battery charge [–]
η_{bd}	Efficiency of battery discharge [–]
η_{syst}	System efficiency [–]

1. Introduction

1.1. Motivation and background

According to the International Energy Agency (IEA), over one third of the global energy consumption, and 40% of the present global CO_2 emissions, originate from buildings and the building construction sector [1]. Reducing the energy consumption related to buildings is therefore important to reach the goal of limiting the global warming to 1.5 °C, as presented by UN's Intergovernmental Panel on Climate Change (IPCC) in 2018 [2].

IEA concretize this need by stating that the share of clean heating technologies must reach 50% of sales by 2030 [1]. Similarly, EU has now set a target of at least 40% of renewable energy sources in the overall energy mix by 2030 [3]. In addition, EU's energy performance requirement for buildings has the goal to achieve a highly energy efficient and decarbonised building stock by 2050 [4]. The Norwegian counterpart is the progressively tightened building standards to passive house level, with the aim to reach zero emission level within the next update of the Technical Standard (TEK 20) [5].

All over the world, government policies are used to encourage houseowners to contribute to this improvement. Some common mechanisms are investment subsidies, electricity price subsidies, feed-in tariffs, and capacity tariffs. Regarding ground-source heat pump (GSHP) systems, Norway no longer subsidizes installing air-to-liquid heat pumps, while liquid-to-liquid heat pumps are still subsidized with up to 1 000 USD [6]. Germany, on the other hand, may subsidize up to 35% of the installation costs of both heat pump types if they meet certain criteria [7]. Germany has also for a long time encouraged the installation of photovoltaic (PV) systems by offering generous feed-in tariffs [8]. As another example, the UK's Smart Export Guarantee (SEG) gives small-scale producers of renewable energy the opportunity to sell their generated electricity to the national grid [9].

Though different, all the regulations and policies push the development towards zero emission energy solutions combining PV systems, batteries, GSHP systems, air-to-water heat pumps, and other generation or storage means. Various government policies will encourage house-owners to design and operate their energy system at various levels of sustainability. With more sustainable energy system usage, energy is not wasted, and the climate change is slowed. Consequently, there is a need to consider the sustainability level achieved from different policies at various surrounding conditions. The present work focuses on detached residential houses, where the energy system consists of PV systems for energy generation and batteries and GSHP systems for energy storage.

1.2. Literature review

Various designs are possible for combining PV and GSHP systems. Sommerfeldt and Madani [10] presented and evaluated several system configurations considering both economical and sustainability issues. Another configuration was recently installed in Norway [11]. Here, energy is stored from solar thermal panels and from excess heat from a heat pump driven by PV energy. The stored heat is used for space heating without the use of a heat pump. Shakerin et al. [12] also looked at combining heating and cooling with a GSHP system, focusing on sizing and on modelling of the heat pump and the hot water tank.

When optimizing the operation of an energy system for a dwelling or an office building, thermal comfort is often used as a criterion. An example is Korkas et al. [13], who considered demand response in microgrids, ensuring the thermal comfort of the occupants. Alimohammedisagvand et al. [14] also considered demand response algorithms for thermal comfort in residential houses, focusing on the hot-water storage tank and on control algorithms for demand response.

Combined optimal design and operation was considered by Williams et al. [15], who addressed self-consumption for different housing standards with different battery capacities and size of the PV system. Salpakari and Lund [16] used a simulation approach to consider a similar setup in a case study for a Finnish low-energy house, restricted to comparing the use of GSHP and battery to shiftable appliances. Litjens et al. [17] discussed a combination of PV, GSHP and battery storage to reduce greenhouse gas emissions using measured demand data from 16 dwellings in the Netherlands. Kavian et al. [18] used a case study in Iran to study such systems from a life cycle analysis point of view.

Mixed-integer linear programming (MILP) is linear programming in which some of the variables are required to be integers. Variables that take integer values might for instance represent the number of Borehole Heat Exchangers (BHEs). A few studies have used MILP to simultaneously optimize system size and demand response. For instance, Beck et al. [19] presented use of residential heat pumps to increase self-consumption of PV energy, while simultaneously sizing PV systems, heat pumps, and storages for various scenarios. In another study, Erdinc et al. [20] considered the optimal sizing of PV and energy storage systems in smart households. They found that the optimal size of both PV and storage systems depend on the feed-in tariffs, as well as on the specific load profiles.

Several of these works addressed energy policies as an aside to their main focus. Litjens et al. [17] discussed the effect of natural gas tariff and electricity tariff, Kavian et al. [18] included scenarios of varying interest rate and inflation rate, and Erdinc et al. [20] considered the effect of feed-in tariffs. On the other hand, the main concern of Sim et al. [21] was the effect of different energy sales mechanisms on the optimal price-energy savings combination for an office building.

1.3. Main contributions of the work

According to the literature review, the influence of government policies on the sustainability level of the design and operation of private houses' energy systems has not been investigated in detail. More specifically, this applies to energy systems consisting of electric and hot water loads, PV systems, batteries, utility, and GSHP systems.

Some of the studies cited do not compare a GSHP with optimal system design to having no GSHP system installed, some do not consider using energy from the PV system to regenerate the borehole, while some do not consider geothermal energy storage at all. Conversely, some do not consider PV energy as an alternative energy source when GSHP usage is considered. Some studies on optimal system sizing do not take demand response into account or do not consider in detail how the GSHP system is operated in an optimal way. Conversely, some studies on demand response do not consider GSHP system size or design. Others treat different system sizes as optimization cases, rather than optimizing the size. Different kinds of government policies are discussed, but in most cases, this is more of an aside than the main focus.

The novel contribution in this study is therefore towards optimizing both energy system demand response and design of GSHP systems at the same time, using PV energy not only to run the GSHP, but also to store energy in the borehole. The sustainability level resulting from varying government policies is discussed, and the resulting optimal energy system operation is investigated in detail.

The approach is demonstrated on a single-family house on the south coast of Norway. The region has a high share of solar hours during the summer and short days with few solar hours in winter. There are significant heating needs during winter, while cooling is usually not installed in Norwegian family houses. Actual registered data of solar irradiation, heating loads, and electricity loads for one year is used. This is combined with prices relevant for the southern part of Norway. Case studies such as these also add valuable insight into the choice and operation of GSHP systems, since, as Hauer and Teuffel [22] argue, energy storage solutions should not be compared in general, but rather for specific systems.

1.4. Paper organization

This paper first describes how the costs and physics of the various components are modelled in Sections 2.1 and 2.2 before moving on to a brief description of the software implementation in Section 2.4. Then follows a case study data set presentation, including prices, loads, and solar irradiation in Sections 2.5 and 2.6.

The optimal design and operation of the energy system are discussed along the following lines:

- Change in energy usage pattern with installation of GSHP system
- Sustainability and the balance between GSHP system benefits and the system's cost
- The dependency of these on various government policies and on physical constraints
- Optimal design of a GSHP system

To investigate these features, one-year simulations of the chosen case study were performed on a few specific simulation scenarios. The scenarios are presented in Section 2.7. The GSHP itself is not studied in detail, rather the effect of BHE depth, of sharing BHEs between houses, and of using an air-to-liquid heat pump for increased energy storage are considered.

Results are presented and discussed in Section 3, before conclusions are offered in Section 4.

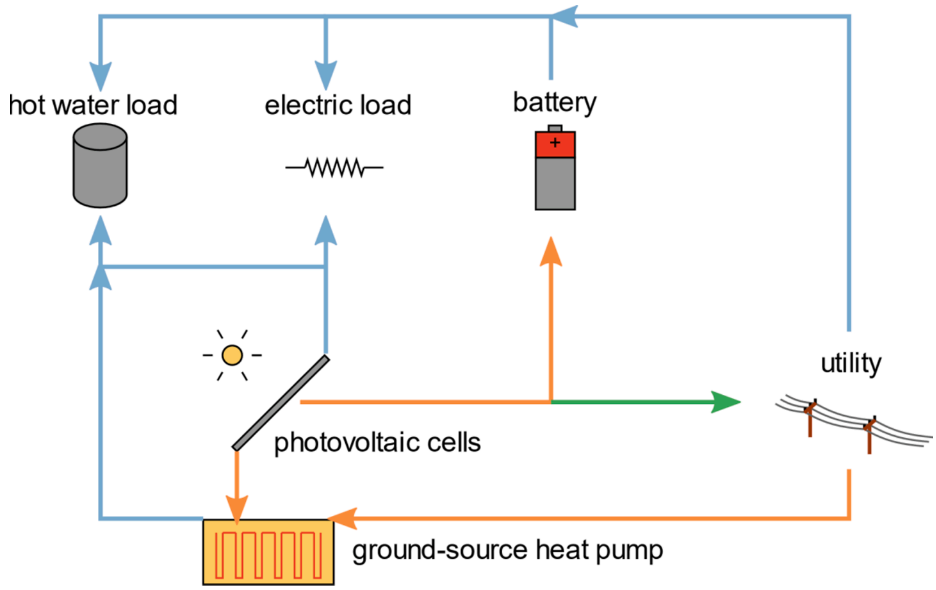

Fig. 1. Energy system overview with hot water loads, electric loads, a battery, photovoltaic cells, a ground-source heat pump, and utility. Blue lines indicate flows to cover loads, orange lines indicate flows to energy storage, and the green line indicates generated PV energy sold to the utility.

2. Method

To investigate the combination of BHE field configuration and demand response management, a minimum of the total energy cost for the single-family house is sought, limited by known loads, production rates, investment costs, electricity prices, etc. The optimization is formulated as a MILP problem [23] with loads, production rates, etc. as constraints. With a linear cost function defined, the optimum must be along one of the constraints or at the intersection of two or more constraints. This problem formulation enables the optimizer to find the optimal combination of system design and operation, and not only the optimal operation for a given design.

The following sections give more information about how the various costs, loads, rates, etc. are modelled.

2.1. Energy system cost – Objective function

The objective function of the optimization is the sum of costs for battery, GSHP, PV system, and utility. Each cost is summed over the chosen simulation time span. These time-based costs are divided into investment costs and operating costs. Investment costs are converted to annual costs using the concept of Equivalent Annual Cost (EAC) [24]. Further details and equations are given in Appendix A, and the actual cost data used in the simulations is described in Section 2.5.

2.2. Energy system physics – Optimization constraints

The energy system of the building considered consists of hot water loads, electric loads, a battery, photovoltaic cells, an optional ground-source heat pump, and utility. The models used for each part are described in the following sections, with further details and equations given in Appendix B. An overview of the system is shown in Fig. 1.

2.2.1. Loads

The loads are divided into electric loads and hot water loads, with the latter being used for both domestic hot water and space heating. The hot water loads can be (partially) covered by the GSHP system, the PV system, the utility, and the battery. The electric loads can be covered from the PV system, the utility, and the battery.

2.2.2. Battery

The battery is modelled as an energy storage with a state of charge (SOC) which is updated every time step.

The energy produced by the PV system can be stored electrically with batteries, and energy from the battery can be used to meet both electricity and hot water loads. It was decided not to allow for storage of electricity from the grid in the battery, meaning the battery cannot be explicitly used for the type of load shifting that is motivated by fluctuations in the utility electricity prices. However, the storage of PV energy will implicitly shift utility purchase to times with lower electricity prices.

Energy loss in the battery is considered by defining separate efficiencies for charging and discharging. Ageing or temperature effects are not considered explicitly. Instead, one optimization scenario was dedicated to the influence of the battery's capacity.

2.2.3. PV system

The available PV output energy is taken from the Skarpnes time series data. No energy loss, ageing or temperature effects have been modelled.

Only excess PV energy can be sold to the grid. In other words, one cannot sell PV energy to the grid for a high price and at the same time buy cheaper electricity from the grid to cover the building's needs. Energy generated by the PV system can be stored in the battery and in the GSHP, and it can be used to cover both electric loads and hot water loads.

2.2.4. GSHP system

The GSHP system consists of the GSHP, a BHE that may or may not be shared between houses, and an optional air-to-liquid heat pump used to increase the energy storage efficiency. In the optimization problem, several GSHP systems are set up, and the optimization forces the system to choose zero or one of these.

In the model, the BHE can be charged by supplying heat from electricity both from the PV system and from the grid utility. Energy from the BHE can only be used to fulfil hot water needs (domestic hot water and space heating). Hereby, the BHE can contribute not only to minimize mismatch in time between energy supply and energy demand, but also to load shifting motivated by fluctuations in the utility el prices.

The BHE can either be charged directly or by use of an additional air-to-liquid heat pump. The latter choice costs more, but it will increase the amount of heat stored.

2.2.5. Utility

The utility availability is limited by the electric grid supplier. It can be used to cover both electric and hot water loads, and energy from the utility can be stored in the GSHP.

2.3. Sustainability metrics

Sommerfeldt and Madani [10] argued that a decrease in financial support for private PV systems will lead to increased focus on energy storage and self-consumption. Self-consumption (SC) and self-sufficiency (SS) as defined by Luthander, Widen, Nilsson and Palm [25] are therefore used for PV system result evaluation.

A high self-consumption means that most of the PV energy generated is consumed in the building itself. This is the main purpose of installing the PV system, so it indicates a good fit between the PV system size and the building's requirements. The grid operators' task to balance the net is complicated by input of PV energy from thousands of small producers. Generating more energy than required on average, indicated by a low self-consumption, is therefore not a benefit for the sustainability of a detached residential building.

A high self-sufficiency means that most of the energy needs of the building is covered by the generated PV energy. Thus, less utility energy is required. In many countries, this directly leads to less use of fossil fuels. For the case study presented here, which is in Norway, the alternative heating source is mostly renewable electricity from hydropower. Reduced utility energy consumption from buildings will then make more renewable energy available for other purposes, where it can replace fossil fuels. A high self-sufficiency therefore indicates a high level of sustainability independent of the alternative energy source for that particular building.

Excess PV energy generation (EPV) is excess energy generated by the PV system, which is neither sold to the grid, stored, nor used directly to cover hot water loads or electricity loads. Non-zero EPV can therefore be seen as wasted energy, while zero EPV indicates a more sustainable energy system. Non-zero EPV occurs due to certain combinations of loads and tariffs in the following situations:

- only PV energy generation exceeding the present demands from the house can be sold to the grid
- there is a limit on the amount of PV energy that can be sold to the grid even with feed-in tariffs
- the optimization does not recommend selling PV energy at zero price, i.e. with feed-in tariff off

2.4. Implementation

The BHE was modelled using the open-source software pygfunction, version 1.1.1 [26], and the optimization was programmed in Python 3.8 using python-mip [27], much as described by Bordin and Mo [23].

The optimization problem is built from the variables and constraints described in the previous sections. The principal variables to be determined are the various power flows – from PV system to battery, from PV system to cover electricity loads, from utility to cover hot water loads, etc. All these variables are vectors, with one item for each time step. For instance, 11 flows simulated over 10 timesteps give $11 \times 10 = 110$ variables that are initially fully independent. Subsequently, constraints are added, giving relations between the variables, e.g. due to limits in battery capacity or in PV energy availability. Each of the GSHP system configurations gives rise to three additional flows plus a discrete variable indicating if that specific GSHP system exists or not. The sum of all the existence variables is limited to be less than or equal to 1, meaning either one or no GSHP system solution is allowed. The resulting problem consists of a set of numerical equations, several equations for each time step.

After minimization of the variable costs, the Python program interprets the results from the optimization as power flows, GSHP existence, etc. Thus, the optimization does not require repeated simulations of the system. To speed up the simulations, one-year simulations can be performed with the integer variables in an outer loop, and the resulting linear programming problems in the inner loop.

The python program developed in this project consists of classes for each of the energy system parts; the battery, the GSHP system, the loads, the PV system, and the utility. There is also a building class, where an object of the building class has objects of the different energy system part classes. Finally, there is a DemandResponseManager class, which is responsible for running the optimization of a given building. All the classes have default parameter values for costs, availabilities, etc., all of which can be replaced by user-chosen values from the simulation's main loop. Data on electricity prices, loads, and produced PV energy are loaded from csv files. When a simulation is finished, utility functions are used to plot the results and to store the results as json files.

A similar study can be performed for any building where one would like to consider the impact of energy policies on optimal energy system operation. For simulating such cases, the corresponding parameter values and csv files must be changed. Larger changes, like allowing electricity from the utility to be stored in the battery, require programming changes.

2.5. Case-study costs

All costs and prices are given in USD, assuming an exchange rate of 10 NOK per USD for costs given in NOK. The cost models for each energy system part are described in the following sections, while details are given in Appendix C.

2.5.1. Battery and PV system

In the present case study, the PV system, batteries, and water-based space heating are assumed to be either already installed or already planned. These investment costs are therefore considered fixed and are not part of the optimization objective. If another case was investigated, these costs would be included in the same way as the GSHP system investment cost. For instance, the cost of the area required for batteries and PV systems may be significant. Even PV systems installed on rooftops may compete with other uses, for instance in an urban environment.

The price per kWh energy produced, stored, or transported is here assumed to be negligible.

2.5.2. GSHP system

GSHP system costs were taken from Traaen [28] and Norsk Varmepumpeforening [29].

2.5.3. Utility

Utility prices were taken from local suppliers relevant for the case study. Capacity tariffs are debated in Norway [30], and presently only implemented for industrial customers or for very large household consumers. Many solutions are possible, e.g. subscribing to a specific capacity and paying for excess peaks, paying for the maximum power peak per month, or for installed capacity. Maximum peak per month was chosen in the present work. The concept encourages peak shaving, thereby giving the consumer an incentive to limit the need for grid expansion.

2.6. Case-study data

Data for the buildings and for the energy system are adapted from the Skarpnes case [31], a small village consisting of single-family houses in the Arendal municipality on the south coast of Norway. Skarpnes was the first zero-energy project for dwellings in Norway [32]. Five of the houses in the village are built as near zero-emission buildings, as a pilot building project within the Research Centre on Zero Emission Buildings

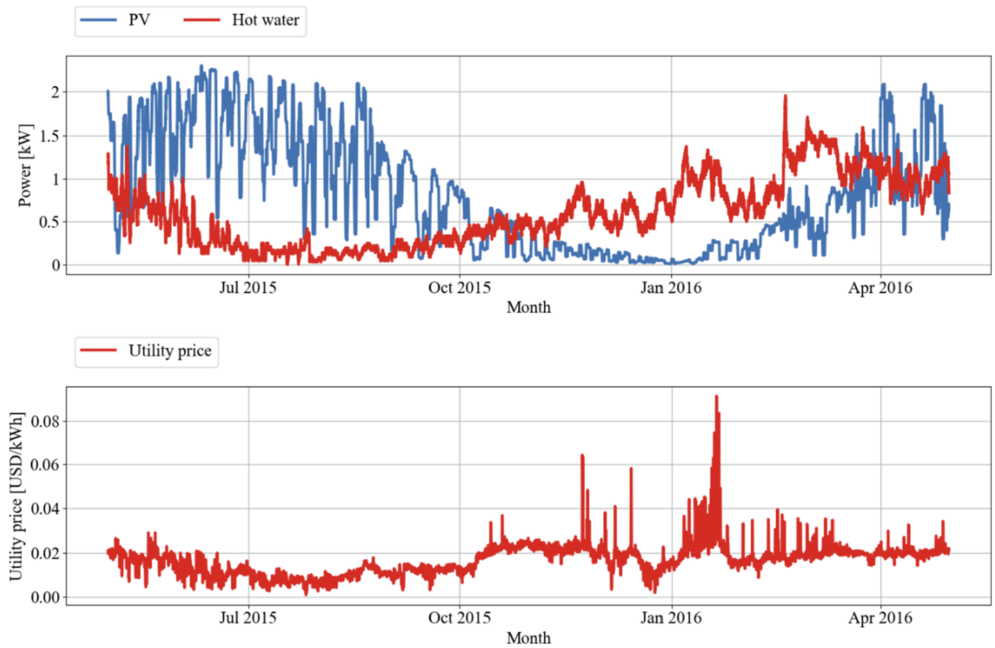

Fig. 2. Running 24-h averages of measured electric PV energy generation and hot water loads per time unit for the year from May 1, 2015 to April 30, 2016 (top) and hourly utility price (bottom).

(ZEB), in a collaboration project between Skanska Norge and SINTEF Community [33]. Further details on the case are given in Appendix D.

PV installation in Norway is increasing rapidly. In 2018, Multiconsult and Asplan Viak performed a study on PV systems in Norway [34]. They found that installed PV power in Norway at the end of 2017 was 45 MWp, a growth of 59% from the preceding year. Scenarios for installed PV power Norway in 2030 vary from 3000 MWp to 6000 MWp, with the highest growth for commercial buildings. The main drivers for private houses were found to be increased technological interest, the need to charge electric cars, independency from the power suppliers, environmental concerns, and reduced expenses. The main hurdles are the investment costs and lack of knowledge. What may be surprising, is that the solar irradiation at the high latitude is not a problem, the solar conditions in Oslo are similar to many European cities, and better than in Berlin.

The five near zero-emission houses at Skarpnes have PV systems, batteries for short-term energy storage, waterborne floor heating, and GSHPs installed. The GSHP is connected to a 100 m deep borehole for each house. In the present study, this GSHP system is used as one possible configuration, comparing this with other possible configurations, as well as with a system having no GSHP installed. The data logged at Skarpnes is also adjusted in some of the simulation scenarios to simulate higher heating loads or higher PV energy generation.

As part of the collaboration project between Skanska Norge and SINTEF Community [32], both energy production and usage data were logged for all five near zero-emission houses. Data for one specific house was chosen since this data set included the most detailed data with the fewest missed samples. The time series used in this study has a resolution of 1 min. From this, the load demand data and the produced PV electricity data are averaged over the chosen simulation time step.

2.6.1. *Time period*

The period of May 1, 2015 to April 30, 2016 was used as a simulation year, interpolating and repeating data when shorter periods of data were missing as described in Appendix E. The peak hot-water load for one minute is 120 kW, while the peak hot-water load for a running one-hour average is 4 kW. The upper plot in Fig. 2 shows 24-hour running averages for PV energy and energy requirements for hot water (used for space heating and for DHW), both per time unit. The uncertainties of these data are found as detailed in Appendix E, and are about 2% for the hot-water load and 1% for the PV generation. The bottom subplot shows the utility energy spot price for the period.

It is to be noted that the measured PV energy generation and the hot water loads are in antiphase with each other, except during the spring months March to May. For the whole period, the total PV energy generated is 7120 kWh, and the total hot water load is 5270 kWh. This illustrates that for houses on the Norwegian south coast the heating needs in the winter can be of the same magnitude as the yearly produced photovoltaic energy.

The utility price in the bottom subplot spikes in the cold weeks of January, when the heat load is also high.

2.6.2. *Electric load*

The tags for electric load from the chosen Skarpnes house contain specific information on the origin of the load, e.g. induction oven top or dishwasher. Electric power used for running the GSHP is not included, while the powers recorded for the other electrical appliances are summarised to obtain the total electric load used in the optimization.

2.6.3. *Hot water load*

All the houses at Skarpnes have GSHP systems installed, and one of the tags logged was the energy flow out of the GSHP. This includes both energy extracted from the BHE and electricity to run the GSHP, and it was used as the total energy requirement for space heating and DHW, independent of source. For the case of no GSHP system installed, it is assumed that this energy required is drawn from the grid utility. No further assumptions are made on how this is achieved.

The Skarpnes houses are near zero-emission houses. This explains why the heat load is only 56% of expected total energy usage for a house built according to the 1997 standards, situated in the south coast of Norway.

2.6.4. *PV energy generated*

Generated PV energy was not registered for the whole time period, so generated PV energy is found from the measured solar irradiation. The relation between the two was found using regression from a period when both data sets were available.

If the optimization method shall be applied to another case, where

Table 1
Summary of the simulation scenario properties.

Scenario	Heat load	Feed-in tariff	Capacity tariff	Comment
S1. Zero	Low	+	–	
S2. Zero, feed-in off, capacity on	Low	–	+	
S3. Zero, feed-in low	Low	+	–	Low feed-in price
S4. Zero, fixed spot	Low	+	–	Fixed consumer price
S5. Normal	Normal	+	–	
S6. Normal, feed-in off	Normal	–	–	
S7. Normal, feed-in off, capacity on	Normal	–	+	
S8. Normal, high PV	Normal	+	–	PV × 1.5
S9. Normal, feed-in off, capacity on, low battery	Normal	–	+	80% battery capacity
S10. Very high	High	+	–	

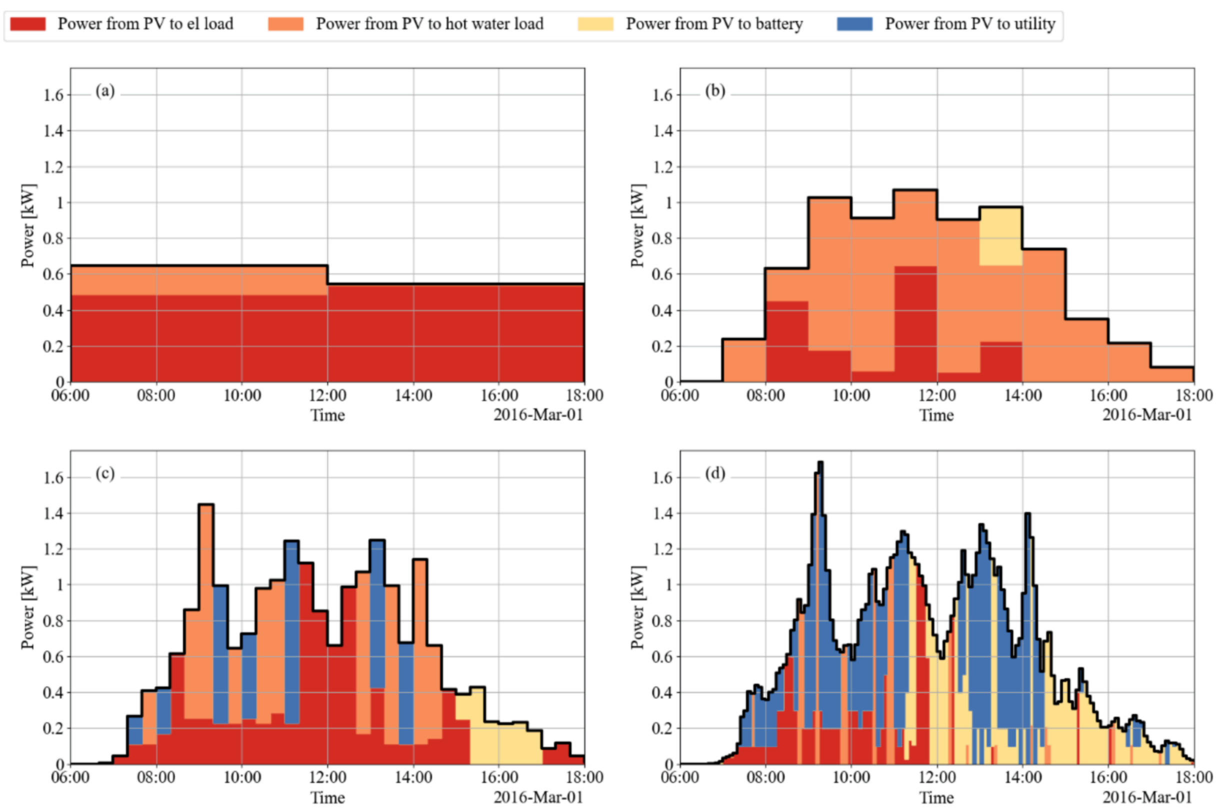

Fig. 3. PV energy usage per time unit for one day in March for time steps (a) 6 h, (b) 1 h, (c) 20 min, and (d) 5 min.

data on PV energy generated is not available, historical solar irradiation data is available from e.g. PVGIS [35]. One can then use information from PV system manufacturers and a chosen PV panel area to transform these data to typical PV energy generation data, similar to the regression approach used here.

2.7. Simulation scenarios

Several scenarios were selected to highlight various aspects that will influence the optimal design and operation of the chosen energy system. One-year simulations with a 1-hour time step were performed for each of these.

Scenario S1 represents the Skarpnes case as it is built, while the other scenarios represent changes, either in electricity tariffs, energy requirements, PV energy generation, battery capacity, or heat pump efficiency.

Since the registered total heat load is lower than for ordinary houses, several scenarios were generated to represent heat loads expected from the 1997 standard [36], which is 107 kWh/m^2, or 16,050 kWh for 150 m^2. This load is designated “Normal”. Note that the 1997 standard is from before the focus on passive construction techniques and zero-emission houses.

The default consumer electricity price contains hourly variations. One scenario with a fixed price for electricity from the grid is added to study the effect of this variation.

Scenarios having feed-in tariff turned off have been included based on discussions by Parra et al. [37] who acknowledged that feed-in tariffs are only a temporary measures, which will be phased out once grid parity is reached, and by Sommerfeldt and Madani [10], who mentioned that financial support for PV systems, including feed-in tariffs, are declining in several countries. Since the default feed-in rate of the case study is higher than the price the consumer pays for electricity from the grid, one scenario with a lower feed-in tariff, set to 0.03 USD/kWh, has also been included.

Scenarios with capacity tariff turned on were included to investigate the effect of heat storage on peak shaving and to reflect the increased focus on capacity tariffs even for single-family houses.

Scenario S8, “Normal, high PV”, is included to investigate the effect of the PV energy generation size, and scenario S9, “Normal, feed-in off, capacity on, low battery”, relates to the effect of an ageing battery.

Scenario S10, “Very high”, with heat load 35 000 kWh per year, is

Table 2
GSHP system choice and costs for one day in March with varying time step size.

Time step	GSHP	Total cost [USD]
6 h	2 deep BHEs shared between 5 houses	4
1 h	2 deep BHEs shared between 5 houses	4
20 min	1 shallow BHE per house	5
5 min	1 shallow BHE per house	7

included based on ENOVA[1]'s recommendation of GSHP for houses using more than 30 000 kWh energy per year [38]. This scenario requires increasing the grid's main fuse from the normal 63 A.

All the scenarios had the same energy storage options available, in addition to the battery and the implicit hot water tanks:

A. One shallow BHE per house with air–liquid heat pump
B. One shallow BHE per house
C. Two shallow BHEs shared between 5 houses with air–liquid heat pump
D. Two shallow BHEs shared between 5 houses
E. Two deep BHEs shared between 5 houses with air–liquid heat pump
F. Two deep BHEs shared between 5 houses

Option B refers to the one available at Skarpnes. Options C – F are included to investigate the option of Community Energy Storage (CES) suggested by Parra et al. [37] and Sommerfeldt and Madani [10]. The optimization could choose one or none of the solutions A-F.

The key properties of these scenarios are summarized in Table 1.

2.8. Time step size

Electricity must be bought to meet load demands that are not met by the PV system. Batteries, selling of excess PV energy generation, and BHEs help to alleviate this problem by storing energy. If a period is simulated by one giant time-step, there is no need to store energy, and electricity from the grid must be bought to cover the difference between total energy produced and total energy demands. As the time step size is reduced, storage becomes useful, and costs may be reduced by storing energy. If, however, the timestep is reduced to a very small value, time differences that arise between supply and demand may not be realistic. In particular, water for space heating can be heated a few minutes earlier or later without any sensible change in comfort or even in room temperature. The electric load demands are harder to delay, but they are much smaller than the heat loads, and thereby do not influence the results as strongly.

This is shown as stacked bars between 6 am and 6 pm for one day in March in Fig. 3. The total bar height represents the total PV energy generation for each time period, and the colors show the usage of power on electric load, hot water load, battery storage, or sold to the grid utility. The corresponding total costs and optimal GSHP system solution is shown in Table 2. The simulations are performed for scenario S5, "Normal".

One BHE per house is more expensive than sharing boreholes between houses, but this solution gives increased capacity. As the time step is reduced, the apparent difference between PV energy supply and hot water demand increases, and higher capacity is beneficial. Since no limit is put on the allowed temperature reduction in the borehole for this short period, none of the cases suggest any energy storage in the BHE, and therefore no air-to-liquid heat pump.

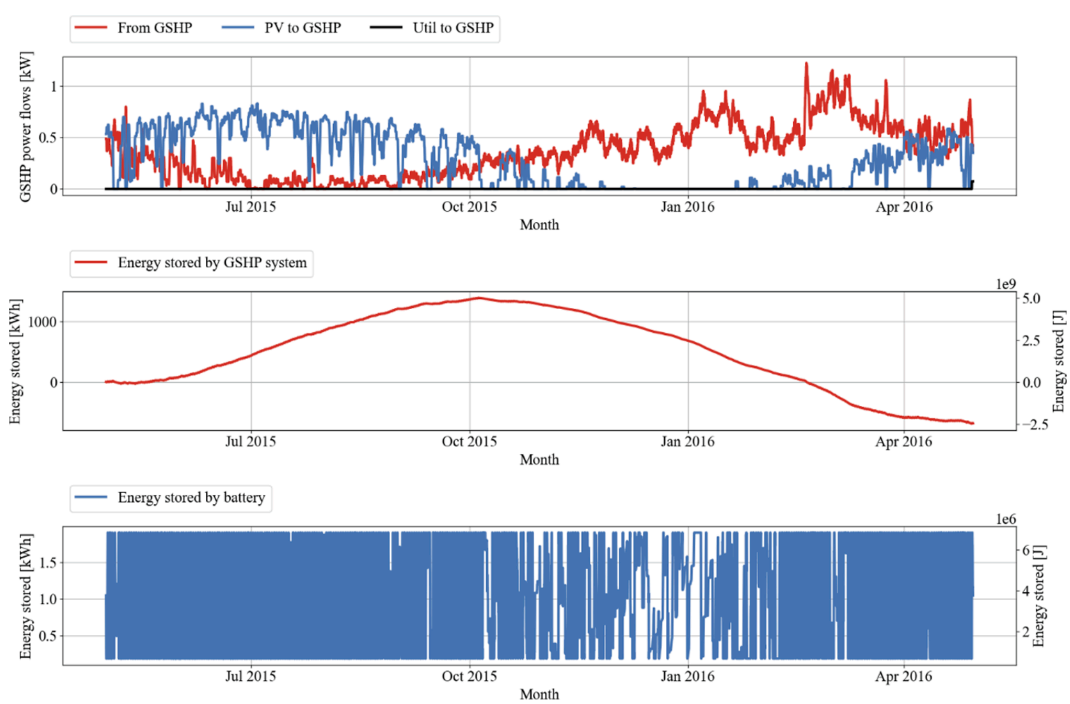

Fig. 4. Running 24-h averages of optimized GSHP usage (top), hourly values of net energy stored by the GSHP system (middle), and hourly values of net energy stored in the battery (bottom). All data is from a simulation of the whole year from May 1, 2015 to April 30, 2016.

[1] ENOVA is a company owned by the Norwegian Ministry of Climate and Environment, working to contribute to reduced greenhouse gas emissions, development of energy and climate technology and a strengthened security of supply

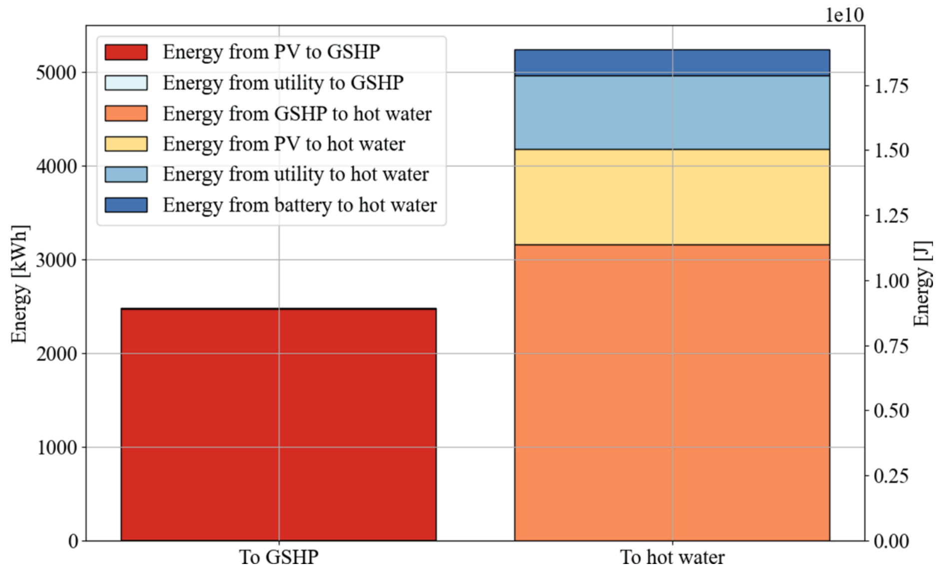

Fig. 5. Aggregated annual values showing energy stored by the GSHP and energy used to cover the hot water load of the house. The energy from utility to GSHP (light blue) is only 0.9 kWh, and therefore hardly visible on top of the energy from PV to GSHP (red).

Since the simulation does not explicitly handle postponing demands, a time step in the range 0.5–2 h is deemed reasonable, similar to what was used by Salpakari and Lund [16].

3. Results and discussion

3.1. Energy usage with a GSHP system

Rationales for energy storage are classified by Parra et al. in their extensive review [37]:

- load shifting, i.e. avoid buying energy when it is most expensive
- peak shaving, i.e. minimizing demand peaks in electricity or heating
- remedying mismatch in time between energy supply and energy demand, e.g. between solar irradiance and heating requirements

Skarphagen et al. [39] emphasize that borehole thermal energy storage (BTES) designs are best suited for seasonal storage. Such storage will therefore most of all reduce the mismatch in time between energy supply and demand.

To investigate the most cost-efficient approach to make use of a GSHP system, the optimization is run for scenario S2, "Zero, feed-in off, capacity on", with 1 h time step. Scenario S2 is different from the original Skarpnes case in that the tariff combination is expected to encourage energy storage in the BHE. However, the cost is higher for a GSHP system installed than without for this scenario. The results presented here are from a simulation where the optimization was forced to choose one GSHP solution. The resulting GSHP usage is shown in Fig. 4.

The upper subplot of Fig. 4 shows running 24-h averages of GSHP usage for the whole year from May 1, 2015 to April 30, 2016. During the sun-rich months from May to September, energy is stored from the PV system (blue line) in the GSHP system. Energy extraction from the GSHP system (red line) gradually increases before becoming dominant in December and January. Energy storage subsequently increases from February onwards. The curves closely follow the time series of total PV energy produced and total hot water loads given in Fig. 2. Since the utility spot price is higher when the heat load is high, more energy is taken out of the GSHP during cold periods both because the heat load is high and because the utility energy price is high. The energy from the utility to the GSHP (black line) remains zero through most of the simulation period, with a small positive value seen at the very end.

In the middle subplot, the power flows shown in the upper subplot are accumulated to represent the net energy stored by the system as a function of time. This can be compared to the energy stored by the battery in the lower subplot. It is seen that the average energy storage time in the BHE is about 6 months, in line with the recommendations for GSHP usage in Skarphagen et al. [39]. Conversely, the battery is typically dis- and recharged daily. It is also to be noted that in the scenario studied here, the existence of a GSHP system effectively increases the energy storage capacity by a factor of about 700.

The battery is less used in January than during other times. Zooming in, it is seen that even then, there are times when the PV energy generation is significant without a matching heat or electricity load. It is then beneficial to tap the battery prior to this period, so it can later be filled with the excess PV energy generation. This behavior is caused by this scenario having no feed-in tariff, electricity from the PV system and from the battery being without extra cost, the small loss on charging and discharging the battery, and that extra energy is always required to extract heat from the GSHP. It would therefore cost more to buy this electricity from the utility, in particular during this high-price cold period.

Very little energy is transferred from the GSHP system during the summer months July and August, as seen in the upper subplot of Fig. 4. This gives the BHE a "resting time", so that the borehole wall temperature does not decrease more than the allowed 0.1 K over a period of one year, even though more energy is extracted from the BHE than is injected. If accumulated over many years, this could pose a problem, but with an undisturbed ground temperature of 8.5 °C as in the present case study, it would take several decades before the freezing point of water is approached.

Fig. 5 shows aggregated values of the energy storage by the GSHP (almost exclusively from PV) and its participation to meet the hot water load of the house for the year simulated.

Only a very small amount of energy, 0.9 kWh, is stored from utility to the GSHP system. Note that more energy is extracted from the BHE than injected. This near-balanced operation, also seen from the middle part of Fig. 4, is typical for GSHPs in the class "Ambient BTES" as defined by Skarphagen et al. [39], as opposed what is defined as "High Temperature BTES". In the latter case, the first few years of operation are used to heat up the ground. After a few years, hot water with temperature in the range 30–60 °C (defined as Medium Temperature Underground Thermal Energy Storage (UTES) by the HeatStore project [40]) or even above 60 °C (defined as High temperature UTES by the HeatStore project) can be extracted. With the present use of one or two BHEs in the

Table 3
Key results from simulation scenarios. Self-consumption (SC), self-sufficiency (SS), the objective value of total optimized cost, and excess PV energy (EPV) both without GSHP and with the optimal GSHP solution for each scenario.

Scenario	No GSHP				Optimal GSHP				
	SC [%]	SS [%]	Cost [USD]	EPV [%]	GSHP	SC [%]	SS [%]	Cost [USD]	EPV [%]
S1. Zero	29	29	230	0	D	29	29	630	0
S2. Zero, feed-in off, capacity on	35	34	990	64	D	70	69	1 380	29
S3. Zero, feed-in low	35	34	640	0	D	30	30	1 050	0
S4. Zero, fixed spot	30	29	180	0	D	29	29	620	0
S5. Normal	33	21	500	0	F	33	21	770	0
S6. Normal, feed-in off	41	25	1 010	58	F	90	56	1 290	9
S7. Normal, feed-in off, capacity on	41	25	1 370	58	F	90	56	1 500	9
S8. Normal, high PV	32	30	410	21	F	52	49	710	0
S9. Normal, feed-in off, capacity on, low battery	39	25	1 400	60	F	90	56	1 540	9
S10. Very high	41	8	2 050	0	B	41	8	1 980	0

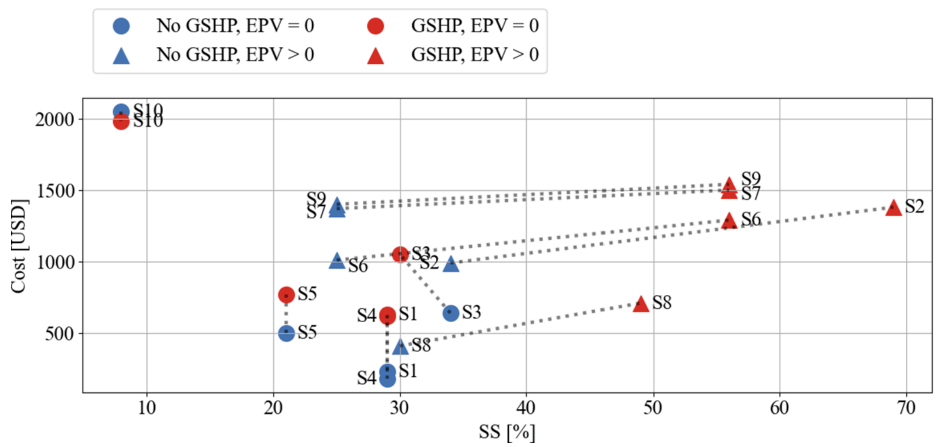

Fig. 6. Energy system cost plotted as a function of self-sufficiency. Each scenario is plotted both with GSHP (red symbols) and without (blue symbols).

optimization stage, the energy loss to the ambient ground will be too large for high temperature operation.

It is also seen that more than half the hot water need, used for both space heating and for DHW, is drawn from the GSHP system in this case. In total, the GSHP system allows for 4447 kWh or 85% of the hot water needs to be met directly or indirectly by PV energy. Without a GSHP system, only 29% of the hot water need is covered by PV energy, either directly or indirectly through the battery. This case therefore illustrates why the energy system sustainability is improved through use of a GSHP system. Even so, for a house with low energy consumption, removing the feed-in tariff and introducing a capacity tariff is not sufficient to make this economically optimal.

3.2. GSHP benefits compared to costs

One-year simulations with 1-hour time steps have been performed for each of the simulation scenarios presented in Section 2.7 Key results are given in Table 3. For each scenario, Table 3 shows simulation results without any GSHP system installed (column 2–5), and with the optimal GSHP system for each scenario (column 7–10). The following simulation results are included:

- Self-consumption (SC), the fraction of PV energy used internally, discussed in Section 2.3 and found from Eq. (14)
- Self-sufficiency (SS), the fraction of the total energy requirement supplied by the PV system, discussed in Section 2.3 and found from Eq. (15)
- Cost: The optimization problem's objective value of total optimized cost, found from Eq. (1)
- Excess PV energy generation (EPV), discussed in Section 2.3

The GSHP system options A–F are defined in Section 2.7 Neither of the options B, D, or F have any air–liquid heat pump for heat storage in the GSHP system. Option B is with one shallow borehole per house, option D is with two shallow boreholes shared between five houses, and option F is with two deep boreholes shared between five houses.

A visualization of the results in Table 3 is shown in Fig. 6, which shows how the self-sufficiency and cost for each scenario change when moving from no GSHP system installed (blue data points) to having the optimal GSHP system for that particular scenario installed (red data points). As seen from Table 3, the self-consumption showed a similar behavior to the self-sufficiency.

The most prominent feature is that for some scenarios, marked as triangles in Fig. 6, the self-sufficiency increases dramatically with a GSHP system installed, resulting in the red data points in the right part of Fig. 6. In other words, an appreciable change in SS is achieved at the expense of a slight increase in cost. For the remaining scenarios, marked with circles in Fig. 6, there is no change in the self-sufficiency when a GSHP system is installed, only an increase in cost.

In all cases except for scenario S10, "Very high", the cost increases if a GSHP system is installed, leading to a vertical shift when moving from blue to red data points. Note, however, that the cost increase is always less than the annual GSHP system investment cost. This is because having a GSHP system installed will result in energy from the BHE being used to cover heat loads, resulting in a reduction of electricity cost, even if none or very little PV energy is stored in the BHE. As discussed in Section 3.1, if the BHE gets a "resting period", for the present case study in Norway, typically during summer, more energy can be taken out of the BHE than is stored.

Looking at the scenarios that show sustainability improvement with a GSHP system installed, it is seen that they have excess PV energy generation without a GSHP system. These are the scenarios without

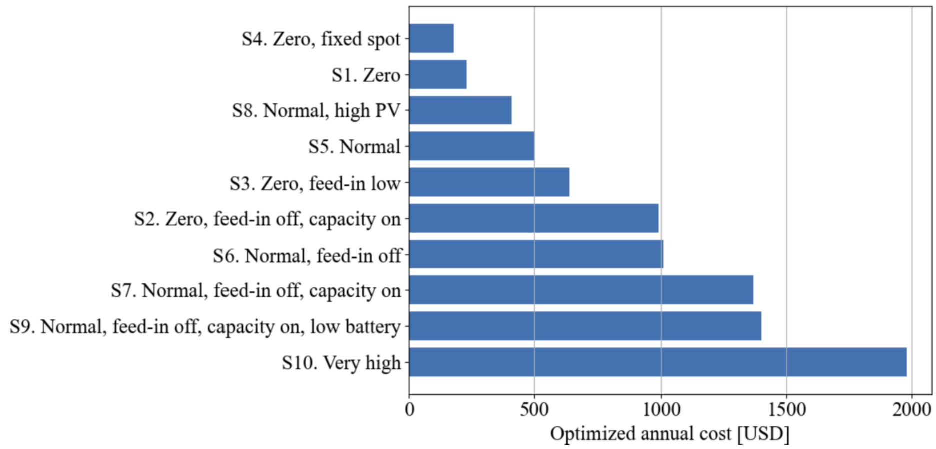

Fig. 7. Optimized annual cost for the ten scenarios.

feed-in tariff or with very high PV energy generation, as seen from Table 3. One of these scenarios is scenario S2, "Zero, feed-in off, capacity on", which was discussed in detail in section 3.1. Here it was seen that the BHE was used actively for energy storage, making PV energy from the summer months available for heating during the winter.

For scenario S1, "Zero", which has exactly the same heating needs as scenario S2, but with a feed-in tariff in place and no capacity tariff, it is more economical to sell the excess PV energy to the grid utility during summer and buy energy from the grid for heating during the winter. With the electricity tariffs used here, this is true even if a GSHP system is installed. In other words, even a free GSHP system will not change how the PV energy is used for this scenario, and thus the line corresponding to S1 in Fig. 6 is vertical. This behavior applies to all scenarios that do not have excess PV energy generation without a GSHP system installed (S1, S5, and S10).

The one exception from the pattern described above is scenario S3, "Zero, feed-in low", which experiences a higher net utility price than scenario S1, "Zero". For both scenarios the GSHP system is mainly used to provide energy to cover the heating demands, with limited storage, enabling more PV energy to be sold to the utility. In contrast to S1, the optimal operation for S3 without a GSHP is to minimize the amount of energy bought from the utility. This behavior results in increased SC and SS when removing the GSHP system.

The lack of economic benefit for GSHP systems found for the present case study is in agreement with ENOVA [38] as well as with Parra et al. [37] and Litjens et al. [17]. The electricity prices in Norway are low compared to prices in other European countries. Higher electricity prices for the consumer will improve the GSHP system profitability and encourage installing more PV capacity. If a feed-in tariff is in place, and this rises in the same way as the consumer prices, the incentive for installing more PV capacity is higher.

In a similar way, if the alternative heating source was fossil fuels, as investigated by Litjens et al. [17], a utility cost can be included in the simulations, also taking into account the negative environmental effect of this source. This approach would further increase the GSHP system's perceived economical usefulness.

The case studied here did not include installed cooling, Only 0.4% of the energy consumption in EU households is used for space cooling [41]. Still, in a few European countries, Greece, Cyprus, Albania, and Malta, the households spend 5% or more of their energy consumption on space cooling [41]. Due to the global temperature increase, an increase in energy-consuming cooling of single-family houses can be expected in many more countries. In Europe, space cooling is almost exclusively covered by electricity [41]. Cooling cost can therefore be reduced by actively using the brine from a BHE to cool the inlet air or to cool the water circulating in the floors or radiators. The resulting heating of the brine can then be used to store energy in the BHE. If so, the net cost for installing a GSHP system will be reduced and the installation may become profitable for single-family houses.

A few modifications are required for the present model to include cooling. The cooling load can be added as a time-dependent load. There is also a need to include efficiency both of the cooling and of the resulting heat storage.

3.2.1. *Electricity tariffs*

The effect of varying electricity tariffs is first analyzed by comparing scenarios S5, S6, and S7 in Table 3, all of which are of type "Normal". Removing the feed-in tariff results in a big change in both cost and in the way the system is run. Even though more PV energy is used for the house itself, reflected as increased self-consumption and self-sufficiency, more than half the PV energy is just excess energy if no GSHP system is installed, and the net energy cost increases dramatically.

The effect of the size of the feed-in tariff is studied by comparing scenarios S1, and S3, both of type "Zero". The latter has a feed-in tariff which is below the price the consumer pays for electricity from the grid. It is seen that without GSHP, this low price makes optimal to store as much PV electricity as possible in the battery in order to buy as little electricity from the grid as possible. The only electricity that is sold to the grid is the energy that would otherwise be in excess. This is seen in that without a GSHP system, it is optimal to run scenario S3 with a low feed-in tariff in the same way as scenario S2, which has no feed-in tariff. It is not optimal to store less PV electricity in scenario S3 than in scenario S2 to sell it for a low price. With a GSHP system installed, the system is run independently of the feed-in tariff size. In other words, the cost of the electricity needed to run the GSHP system is so high that it is better to sell some of the PV generated energy than to store it in the GSHP. Note how the lower non-zero feed-in tariffs directly reduces the economic benefits of the PV panels.

The effect of feed-in tariffs is also seen on scenario S2, "Zero, feed-in off, capacity on". The EPV of 29% even with a GSHP system is a result of the PV system generating more energy than the house can make use of. This shows that counting on the profitability of feed-in tariffs when sizing a PV system is not to be recommended, but that such systems should be sized to generate approximately the same amount of energy as the house will require.

With a capacity tariff, the system runs in much the same way as without capacity tariff, only with higher cost. Note that even though seasonal energy storage in a BHE is still not profitable, the cost increase from inclusion of a capacity tariff is much smaller with a GSHP system installed than without.

Fig. 7 shows the optimized annual cost for the ten scenarios. With the exception of scenario S10, this corresponds to the cost without a GSHP system installed. It is observed that scenarios S2 and S6 have about the same cost, even though scenario S2 only has 56% of the heat load of

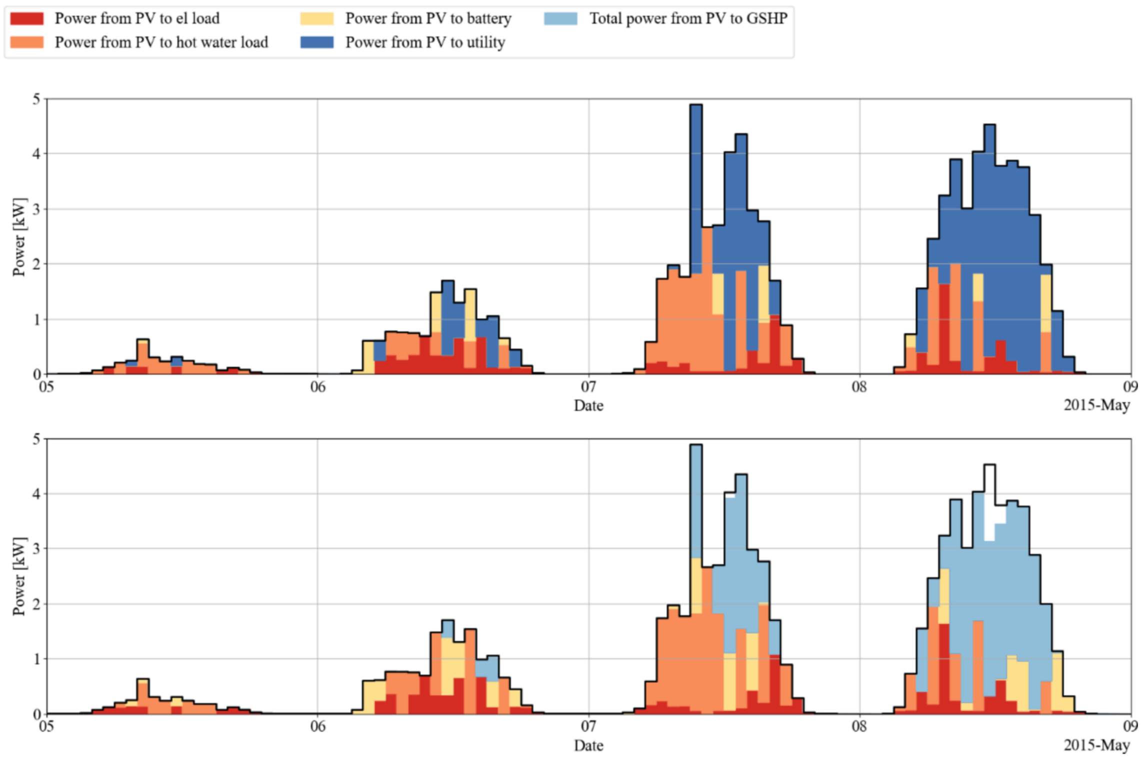

Fig. 8. PV usage for 4 days in May for scenarios S5, “Normal” (top) and S6, “Normal, feed-in off” (bottom).

scenario S6. This is because scenario S6′s feed-in tariff allows for excess PV energy to be sold to the grid utility, which is not possible in scenario S2. Also note the large cost increase from scenario S6 to S7, due to the inclusion of a capacity tariff. Scenario S4 with a fixed spot price resulted in a slightly lower price than with the varying spot price, and the low feed-in price of scenario S3 placed scenario S3 between scenarios S1 with a high feed-in price, and S2 with zero feed-in price and a capacity tariff.

Scenarios S5, “Normal” and S6, “Normal feed-in off” have the same energy load, the same PV energy generation, and the same battery capacity, while they differ in the energy tariffs. To illustrate the differences in the resulting demand response management, the stacked bars in Fig. 8 indicate the usage of PV energy for a few days in May for the two scenarios with a GSHP system installed. Both scenarios are run with 2 deeper boreholes shared between 5 houses, corresponding to energy storage option F.

As expected from the feed-in tariff, PV energy is sold to utility in scenario S5, “Normal” (dark blue bars) and not in scenario S6, “Normal feed-in off”. In the latter scenario, excess PV energy is rather stored to the BHE (light blue bars). Indeed, scenario S5 relies almost solely on limiting the BHE usage to keep the temperature of borehole flow out acceptable, while storing only a modest amount of PV energy. In addition, scenario S5 uses some electricity from the grid to keep the borehole temperature close to constant. The result of these two tactics is that scenario S6 has a higher Coefficient of Performance (COP) for the GSHP, and therefore slightly less electricity is used to meet the hot water demand when the GSHP is used.

In most simulations presented here, the electricity price is based on the spot price. As discussed in Section 2.6.1, this has a tendency to have a high seasonal covariance with the heat load. In other words, cold days require more heating, which also costs more. Scenario S4 can be compared to scenario S1 to see the effect of a constant electricity price. The constant price in scenario S4 is about the same as the average sport price over the simulated year. As seen from Table 3, this change hardly influences the costs or the sustainability metrics. Zooming in on the second (cold) week of January, it is seen that the battery is used much more actively if spot prices are used. This is explained by the high spot price often seen after sunset.

The selections available for PV and utility energy are also influenced by policy choices that are not simulated here. Two examples are no limit on the yearly amount of electricity sold to the grid or allowing other than excess PV energy to be sold to the grid. The limit on the yearly amount of electricity sold to the grid is commonly seen as a hurdle for further installation of PV systems in Norway [34]. Removing this limit would have an effect for scenario S8, “Normal, high PV”, where it would eliminate the EPV and reduce the energy storage benefits. This can also readily be simulated with the present model by changing the corresponding parameter.

Finally, allowing the house-owner to sell PV electricity at the same time as buying electricity from the grid to cover the house’s energy needs would only influence the optimization when the feed-in tariff is higher than the utility price. Even if that is the case for the present study, this is expected to be very rare in the future, as argued by Sommerfeldt and Madani [10]. This situation would reduce EPV and encourage energy storage. To simulate this would require removing the corresponding constraint.

To summarize, feed-in tariffs are seen to discourage local seasonal energy storage. This policy thereby contributes to decreasing the building’s self-sufficiency and self-consumption. This is in line with what was discussed in relation to Fig. 6, where a feed-in tariff could result in even a free GSHP system not changing how the PV energy was used. On the other hand, feed-in tariffs encourage the installation of PV systems without requiring seasonal storage. The effect of these tariffs should therefore be investigated thoroughly before changes are made for private households. The method presented in the current work can be useful and flexible for such considerations.

Beck et al. [19] and Erdinc et al. [20], having considered only smaller storages like batteries and hot water tanks, came to different conclusions on the dependencies of the optimal size of heat pumps and storages on electricity tariff. This suggests that each example case should be considered separately, as was also recommended by Hauer and Teuffel [22].

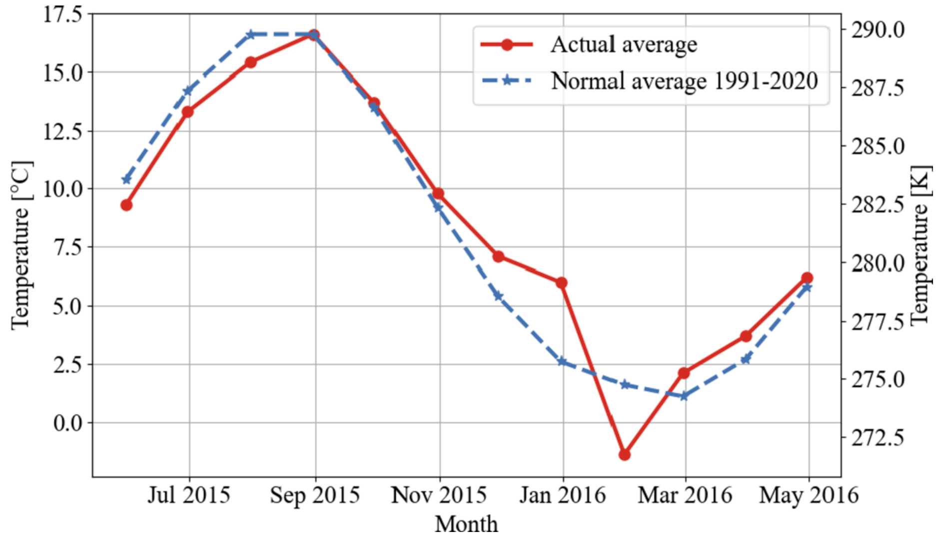

Fig. 9. Monthly average temperatures for Arendal [46,47].

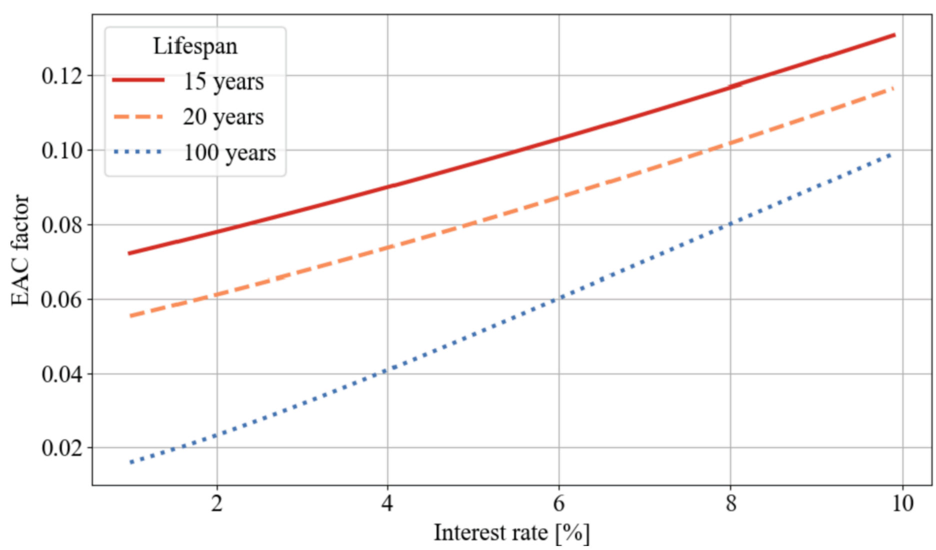

Fig. 10. The dependency of Equivalent Annual Cost (EAC) on interest rate and lifespan.

3.2.2. *Battery age*

Scenarios S7 and S9 are both of the type "Normal, feed-in off, capacity on", but scenario S9 has 80% of the original battery capacity, an example of a consequence of battery aging. Since the system of scenario S9 utilizes less of the PV energy generated, there is a small reduction in self-consumption, directly related to the small increase in wasted excess PV energy and in price. The resulting reduction in self-sufficiency is less than 1%.

The battery age, modelled as reduced battery capacity, is therefore seen to have only a weak influence on the energy system's sustainability, on the total energy cost, on the optimal GSHP system design, and on optimal use of a GSHP system, if installed.

3.2.3. *Heat load*

As expected, it is seen from Table 3 that on increasing the energy requirement from scenario S1, "Zero" to scenario S5, "Normal", the self-consumption and the total cost increases, while the self-sufficiency decreases. The trend is further strengthened when increasing the heat load dramatically to scenario S10, "Very high". The heat load increase results in a very high self-consumption and price, combined with a low self-sufficiency, even with a GSHP system. This illustrates how the sustainability metrics SS and SC may move in opposite directions if there is a mismatch between the amount of energy generated and required. Scenarios S1 and S2 are mostly in line with the current focus on zero-emission buildings, making them the best representatives for new and future buildings.

3.2.4. *PV energy generation*

In scenario S8, "Normal, high PV", the simulated PV energy generation is increased to 1.5 times the generation actually logged at Skarpnes. Otherwise, this scenario's parameters are identical to those used in scenario S5, "Normal". Without a GSHP system installed, the increase in the PV energy generation results in a small reduction in self-consumption, since the PV energy availability is now more often higher than the demand. As expected, the self-sufficiency increases, with a corresponding price reduction. As opposed to scenario S5, a significant fraction of the PV energy is wasted as excess energy in scenario S8, since there is a maximum limit on PV energy sold to the grid.

With a GSHP system installed, the increased PV energy generation leads to significant increases in both self-sufficiency and self-consumption, related to significant changes in energy usage and thereby significantly improved sustainability of the system. There is however a smaller change in optimized cost compared to the case without a GSHP system.

Note that this is a moderate change in PV energy generation, and more radical changes can be expected to have a stronger influence.

3.2.5. Air-liquid heat pump efficiency

An additional simulation of scenario S5, “Normal” was run where the air-to-liquid heat pump COP was increased from 2.7 to 3.5. It was seen that for this scenario, it was not cost-effective to include this heat pump even if its efficiency was increased. The reason is the high price of this heat pump compared to the benefit of storing slightly more energy in the BHE. Even with COP 3.5, the total cost for the simulated year with this heat pump was close to twice the cost of the cheapest solution without it.

3.3. Optimal GSHP system design

It is seen from Table 3 that none of the three GSHP system designs that were found to be optimal, included the optional air-to-liquid heat pump. The purpose of this heat pump was to increase the energy storage efficiency. The difference between the remaining three options without the optional air-to-liquid heat pump is mainly in terms of maximum capacity for heat injection and extraction per time unit, and this choice is found to depended on heat load only. For the near zero-emission scenarios S1 and S2, the solution with the lowest capacity, 2 shallow BHEs shared between 5 houses, was chosen. For scenario S10, “Very high” the solution with the highest capacity, one BHE per house, is chosen. Between these extremes, for the normal heat load scenarios S5–S9, the medium-capacity solution of two deep BHEs shared between 5 houses was chosen.

The sharing of BHEs between houses was discussed by Parra et al. [37], who argued that CES, where several boreholes together comprise a BHE field, give better economy than one BHE per house. This is due to less spiky demand profiles and economies of scale, as well as the option of professional management. Note however, that if the BHEs are used only for heating, there is a risk of interference and reduced efficiency if they are placed too closely together. This community-scale solution is also recommended by Sommerfeldt and Madani [10], on the basis of reduced energy dissipation to the ground.

The findings from the present case study are therefore in accordance with the recommendations by Parra et al. [37]. In practice, one BHE per house may be economically favorable even for the normal heat load scenarios S5 - S9, since the price difference from the shared option is small, and the costs for these shared solutions do not include extra piping. On the other hand, the prices used do not take all the CES benefits into account, such as a professionally run system or less spiky demand profiles.

3.4. Considerations for adding a GSHP system

EU has passed 2 GWth for geothermal heating systems [42]. This is far from evenly distributed between the European countries, and the countries with the highest power installed are Iceland, Turkey, and France [42]. Geothermal heat pumps are particularly ubiquitous in Sweden, with about 130 geothermal heat pumps installed per 1 000 households in 2019 [42]. This contributes to making derived heat the main source of space heating in Sweden [41]. The next country on the list, Finland, had less than half of that, about 60. Norway, where the present case study is from, had about 25 heat geothermal heat pump units installed per 1 000 households in 2019 [42]. Here, the direct use of geothermal energy is estimated to 3.0 TWh, which represents 30% growth since 2015 [43].

One of the questions that motivated the present study was to find out what will encourage the installation of a GSHP system in a single-family house. Based on the analysis presented in the preceding sections, the answer can be divided into two; as seen from a strictly economical point of view or as seen from a wider sustainability point of view.

Economically, a GSHP system is only useful for the single-family house in the case studied if the heating requirements are very high, if the electricity prices rise significantly from the low prices enjoyed in 2015–2016, or if the house has a cooling requirement. The presence of feed-in tariffs is seen to reduce any economic benefit of a GSHP system installation. However, even without any feed-in tariffs, there is a net cost increase from adding a GSHP system, as long as the heating requirements are normal or small. Installing a GSHP system will result in a close to constant inlet temperature to the heat pump used to heat water for both DHW and for space heating. This is a lesser economic benefit not investigated in the present study, but it will increase the lifetime of the heat pump, thereby reducing maintenance costs.

In terms of sustainable energy production and consumption, curtailing substantial amounts of PV electricity should be avoided. Consequently, a GSHP system is also recommended whenever analyses suggest that there is a high probability of significant excess PV energy generation. This can happen if feed-in tariffs are likely to be removed during the lifetime of the house or if the PV energy generation is higher than required to meet the heating needs. Alternatively, small amounts of excess PV energy can be eliminated by increasing the battery size or by using the excess to charge an electric vehicle.

Renewable energy extraction using a GSHP is particularly favorable if heating loads are otherwise covered through nonrenewable sources such as gas or coal. Regardless of whether PV energy is stored in the ground using the BHE, a GSHP will reduce the external energy requirements, thereby reducing greenhouse gas emissions. As discussed previously, this argument applies even if one particular house or region has renewable utilities available. Options should therefore be considered in such regions for making GSHP systems economically profitable for single-family houses.

Possible negative environmental impacts from installing a GSHP system include changes to the ground water and to the geological features [44], as well as to the above-ground environment from e.g. foul smell and noise [45]. Investigations show that GSHPs have only minimal effect on the environment because they are shallow (100–200 m) and the temperature changes are small [45]. It has also been concluded that GSHPs are safe and sustainable if care is taken during planning, installation, and operation [44]. Consequently, policy makers need not be concerned about negatively influencing the environment by encouraging GSHP installation.

3.5. Limitations

3.5.1. Input data to the simulations

There are large ranges of missing data and uncertainties in the Skarpnes data. This means that the solar irradiation data is often not from the same actual dates as the load data. Significant parts of the data are also interpolations, replacements, or averaged values. Still, the used data set indicate a higher demand for heating in winter than in summer, shorter periods of sunshine in winter than in summer, and a realistic distribution of sunny and cloudy days. For each day, the load distribution typical for single-family houses is also preserved with higher loads in the morning and evening. Therefore, the dataset used here presents a relevant example of a single-family house in the southern part of coastal Norway in recent years.

The uncertainty in the data for generated PV electricity is discussed in detail in Appendix E. The data is only used to exemplify a new, near zero-emission house on the south coast of Norway. Consequently, the error corresponds to a slightly different set of solar panels or a year with slightly different weather conditions. Finally, the similar optimal GSHP system designs for scenarios S5, “Normal” and S8, “Normal, high PV” indicate that the optimal GSHP system design is not strongly dependent on the amount of PV energy produced.

Even though the average temperature for the chosen year, 8.5 °C [46], is very close to the normal average for the period 1991–2020, 8.3 °C [47], the chosen year had a colder February than normal, as seen in Fig. 9. This cold month will somewhat increase the usefulness of a GSHP system in this particular year relative to the average year.

According to PVGIS [35], the solar irradiation at Arendal in the ten years preceding the simulation period, i.e. 2007–2016, varied from 880 to 1030 kWh/m^2, with a standard deviation of 5% of the average value for the period. For the simulated time period, PVGIS' data indicate a total solar irradiation of 995 kWh/m^2, i.e. at the average for the 10-year period.

Simply dividing the battery capacity by the number of houses does not take the community effect into account. However, all houses experience the same weather, and thus similar solar irradiation and similar heating needs. The approximation is therefore justified since the focus of the case studied is not battery dimensioning. Very similar results were obtained for scenarios S7, "Normal, feed-in off, capacity on" and S9, "Normal, feed-in off, capacity on, low battery". The latter had 80% of the battery capacity of the former. This finding indicates that the exact battery capacity is not important for the optimal GSHP system design, nor for other key metrics such as self-consumption, self-sufficiency, or excess PV energy.

3.5.2. Interest rate and asset lifespan

The investment costs are converted to annual costs using EAC. As shown in Eq. (6) in Appendix A, this conversion depends on the interest rate and on the estimated lifespan of the assets. Since the energy systems parts all have long lifespans, the effect of changing the interest rate is significant, and the interest cannot be expected to be constant.

The EAC factor's dependency on these two factors is plotted in Fig. 10.

The close to parallel lines in Fig. 10 indicates that the two factors lifespan and interest rate can be considered independent of each other

It is seen that an increased interest rate will increase the total cost, but the ratio between the costs of two different GSHP systems with different investment costs will not be influenced. The interest rate therefore does not influence which GSHP system is the optimal one. However, the interest rate will affect whether installing even the best GSHP system will be cost worthy.

This argument can also be used if the interest rate varies over time, since it will vary in the same way for all the possible GSHP systems. If the more short-lived optional air-to-liquid heat pump experiences a lower average interest rate than the long-lived borehole does, this will make the options with this heat pump less expensive than presently assumed. However, the cost differences are so big that this is not likely to influence which GSHP system is optimal.

A similar argument can be made for the estimated lifespan of a GSHP system. If 50 years is a better estimate for the lifespan of a borehole than the default 100 years, the total annual costs will increase, and it will be less profitable to install all GSHP systems.

3.5.3. BHE design

As mentioned in Appendix B, an approximation for the fluid temperature leaving the borehole is used during optimization. After each optimization, the difference between the average fluid temperature during BHE discharge and the average approximated temperature was calculated. If this difference was more than 0.1 K, the optimization was rerun with a corresponding parameter change. However, this rerun never changed the resulting optimized cost more than a few USD. This is in correspondence with the Carnot efficiency of the liquid–liquid heat pump not being significantly influenced by small changes in this temperature, going from e.g. 281.5 to 280.3 K only changes this efficiency from 7.1 to 6.9.

The maximum BHE capacity was found to be important for its design. In the present model a fixed maximum capacity in W per m borehole was used. The resulting temperatures of fluid and borehole walls were then calculated using pygfunction [26]. In a more advanced model, these temperatures could be used together with the known brine flow rate to verify if it was possible to inject or extract the desired amount of energy to or from the BHE over the chosen time span.

3.5.4. Model assumptions

A constant efficiency of battery charging and discharging is a simplification. A too low estimated battery efficiency will reduce the importance of the battery, increasing the perceived usefulness of a GSHP. This effect is reduced by the GSHP primarily being a seasonal energy storage, while the battery is primarily used for short-term storage. The discussion of battery age showed that a reduction of the battery capacity to 80% had very little influence on the results. This indicates that only significant battery efficiency changes would have a strong influence on the qualitative results.

A temperature dependency of the battery efficiency can be added directly if temperature measurements are available. Alternatively, a time dependency can be used, based on known typical seasonal temperature variations. Since the present model always knows the source of energy entering the battery, it would be straight-forward to add a dependency on the charging medium. However, both these kinds of dependencies would introduce their own uncertainties.

The model does not allow for storage of electricity from the grid to the batteries. This model assumption influences the choice between PV or utility energy for covering loads and for storage, and it thereby represents a policy choice that could be further explored. The model uses hourly utility prices, so the option to store energy from the utility to the battery for short-term energy storage would be a cost-saving opportunity. In the present case study, the battery is completely charged and recharged most days, so an increased battery capacity would probably be required. This extra cost could then be weighed against the benefits.

The maximum power that can be stored or retrieved from the GSHP is limited by the borehole in the present model. The liquid-to-liquid heat pump capacity is always assumed to be sufficient. The heat pumps contribute significantly to the GSHP system cost, and their cost depends strongly on the rated power. If a smaller heat pump than specified would be sufficient, the cost of the GSHP system is therefore overrated. Since most scenarios simulated showed that installing a GSHP system would not be cost-efficient, the opposite problem, that a heat pump of the rating simulated is too small, will not influence the results as strongly.

3.5.5. Software choices

The g-function library by Cimmino is evaluated against the numerical g-function calculation from 1988, as referenced by Cimmino [26]. It has also recently been tested by Spitler et al. [48], who found excellent accuracy for small borehole fields, up to 20x10.

The optimization tool chosen, python-mip [27], is a common documented open-source tool. The packages' authors have used it for their research publications, and the solver used, CBC, is a standard solver. Both the python package and the CBC solver are parts of the COIN-OR project [49]. The results obtained are therefore considered trustworthy.

3.6. Method application

The authors believe the method presented here can be used for policy makers to evaluate the effect of their policies on private house energy systems, both on designs and on operation schemes. The resulting design and operation can then be evaluated both in detail and for overall sustainability. As the discussion on e.g. feed-in tariff shows, the net result is often the consequence of balancing several effects, and not always easy to predict.

Conversely, the method can be used to consider the sensitivity of a specific case towards policy changes. One example could be to know what will happen to a house's energy cost and self-sufficiency if a capacity tariff is introduced, or if a feed-in tariff is removed or greatly reduced.

The optimal operation found may also serve another purpose, since it can be used as an upper bound for testing the performance of demand response algorithms. These real-life algorithms will not have perfect knowledge of the loads and power generation for a whole year, so they will have poorer performance. However, a good demand response algorithm will come close to the results found by the method presented here.

4. Conclusions

The present work considers optimal design and operation of private house energy systems. These energy systems are assumed to consist of photovoltaic systems for energy generation and batteries and optional ground-source heat pump systems for energy storage. The goal is to investigate the resulting sustainability, to learn how it will depend on local energy policies and on other factors.

A mixed-integer linear programming model is presented, which takes policies and other surrounding conditions into account and optimizes system size and operation. The results relate overall sustainability validation to parameters such as self-sufficiency and self-sustainability, as well as a detailed drill-down of the optimal operation. Simulations were performed for a case study in Norway over a period of one year with one-hour time steps.

Two modes of ground-source heat pump usage were seen. With a feed-in tariff present, its main use was as an energy source, while without this tariff the optimal use was for seasonal energy storage. Neither the exact amount of photovoltaic energy available nor the exact battery capacity were found to have a strong impact on the optimal ground-source heat pump system design or on the energy cost for a given tariff system. However, the economy and sustainability of an energy system with a significant mismatch between energy generation and energy loads were seen to be very sensitive to feed-in tariffs. It was also found that ground-source heat pump systems contribute to increased sustainability, but they may not be economically beneficial for single-family homes with low or medium heating requirements.

Demands for heating and cooling change with time and place, as do available area for photovoltaic energy generation and externally available energy sources. Therefore, a detailed analysis of the kind presented here is recommended before new energy policies are implemented. For each specific house or project, this kind of analysis will also be useful to evaluate the sensitivity of an energy system's performance to changing policies.

CRediT authorship contribution statement

Ellen Nordgård-Hansen: Conceptualization, Methodology, Software, Investigation, Data curation, Writing – original draft, Writing – review & editing, Visualization, Project administration. **Nand Kishor:** Methodology, Writing – review & editing. **Kirsti Midttømme:** Conceptualization, Resources, Writing – review & editing, Project administration, Funding acquisition. **Vetle Kjær Risinggård:** Investigation, Writing – review & editing. **Jan Kocbach:** Conceptualization, Methodology, Software, Writing – review & editing.

Declaration of Competing Interest

The authors declare that they have no known competing financial interests or personal relationships that could have appeared to influence the work reported in this paper.

Acknowledgement

Professor Huynh Van Khang at the University of Agder is acknowledged for valuable discussions during the work with this project.

Funding: This work was supported by the Research Council of Norway [grant number 285545]

Appendix A. Details on energy system cost

The objective function of the optimization is given by Eq. (1)

$$c_{tot} = c_b + \sum_i c_{GSHP_i} + c_{PV} + c_{util} \tag{1}$$

where the subscripts to costs c indicate cost source, with b for battery, $GSHP_i$ for GSHP system number i, PV for PV system, and $util$ for utility.

The individual terms in Eq. (1) are given by Eqs. (2)–(5)

$$c_b = c^{b,e}_{b\rightarrow el} + c^{b,e}_{b\rightarrow hw} + c^{b,t} \tag{2}$$

$$c_{GSHPi} = c^{GSHP_i,e}_{GSHP_i\rightarrow hw} + c^{GSHP_i,t} \tag{3}$$

$$c_{PV} = c^{PV,e}_{PV\rightarrow el} + c^{PV,e}_{PV\rightarrow hw} + c^{PV,e}_{PV\rightarrow b} + c^{PV,e}_{PV\rightarrow util} + c^{PV,t} \tag{4}$$

$$c_{util} = \sum_i c^{util,e}_{util\rightarrow GSHP_i} + c^{util,e}_{util\rightarrow el} + c^{util,e}_{util\rightarrow hw} - c^{util,p}_{PV\rightarrow util} + c^{util,c} + c^{util,t} \tag{5}$$

For each cost term in Eqs. (2)–(5), superscript indicates the type of cost, while subscript indicate the origin of the cost, e.g. $b\rightarrow el$ indicate the power flow from battery to feed the electric load. Cost types are represented as e for energy costs (USD/kWh), t for time-based costs (USD/year), p for profit (only used for selling PV energy to utility), and c for capacity cost (typically based on peak flow).

The equivalent annual cost is the annual annuity payment incurred each year of the project lifetime to cover the initial investment. The EAC can be used to compare investments for two or more projects with different lifespans and is given by Eq. (6)

$$EAC = I\cdot\frac{r}{1-(1+r)^{-m}} = I\cdot\frac{r(1+r)^m}{(1+r)^m-1} \tag{6}$$

where I is the investment cost, r is the interest rate, and m is the number of years the equipment is expected to last. In the present project, the interest rate is default set to 5%.

Appendix B. Details on energy system physics

This section gives details and equations for how the energy system parts loads, battery, PV system, GSHP system, and utility were modelled.

For energy storage, the building in the case study also has one hot water tank of 185 l for domestic hot water (DHW) and one of 40 l for floor heating. These tanks cause less spikes in the registered data of hot water consumption, but they are not modelled explicitly as energy storage in the present work.

Loads

All load demands must be met at each time step, giving the optimization constraints in Eqs. (7)–(8)

$$f_{PV\to el}(n) + f_{util\to el}(n) + \eta_{bd} f_{b\to el}(n) \geq l_{el}(n) \tag{7}$$

$$f_{PV\to hw}(n) + f_{util\to hw}(n) + \eta_{bd} f_{b\to hw}(n) + \sum_i f_{GSHP_i\to hw}(n) \geq l_{hw}(n) \tag{8}$$

where f are power flows with subscripts indicating source and sink, l are load demands, n is time step number, η_{bd} is the discharge efficiency of the battery, and i is GSHP number.

Battery

The total battery capacity of all five houses in the Skarpnes case is 9.5 kWh. The battery of each house is modelled as a simple energy storage with capacity of 9.5/5 = 1.9 kWh and a minimum state of charge of 10% of this, to avoid premature cycle degradation.

Energy loss is considered by defining separate efficiencies for charging and discharging, η_{bc} and η_{bd}. The default values give a total round-trip efficiency of 92%, the efficiency used by Litjens et al. [50], i.e. $\eta_{bc} = \eta_{bd} = \sqrt{0.92}$. This is a simplification, where temperature effects or how the efficiency depends on the charging medium are not taken into account.

At each time step except the first, battery usage gives the optimization constraints given in Eqs. (9)–(10)

$$\mathrm{SOC}(n) = \mathrm{SOC}(n-1) + dt\cdot(\eta_{bc} f_{PV\to b}(n-1) - f_{b\to el}(n-1) - f_{b\to hw}(n-1)) \tag{9}$$

$$\mathrm{SOC}_{min} \leq \mathrm{SOC}(n) \leq \mathrm{SOC}_{max} \tag{10}$$

where $\mathrm{SOC}(n)$ is the state of charge at time step n, f are the power flows with subscripts indicating source and sink, and SOC_{min} and SOC_{max} are the limits for state of charge. This is an energy balance. As seen in the list of symbols, the unit of SOC is J, which may be converted to Wh for presentation. The power flows are in W, and the time step length in seconds.

The initial state of charge is a parameter chosen by the user, and the state of charge at the end of a simulation period is constrained to be equal to this initial state, to avoid "free" battery usage, as shown in Eq. (11)

$$\mathrm{SOC}(N) = \mathrm{SOC}(0) \tag{11}$$

where N is the final time step number.

To speed up the optimization, auxiliary variables are defined for SOC, with upper and lower bounds given by Eq. (10).The battery's total availability was default set to 5 kW, as suggested by Litjens et al. [50] and as offered by Tesla in their Tesla 2 Powerwall [51], leading to 1 kW availability for one house.

PV system

The optimization constraint describing the available PV power is given in Eq. (12)

$$f_{PV\to el}(n) + f_{PV\to hw}(n) + f_{PV\to util}(n) + f_{PV\to b}(n) + \sum_i f_{PV\to GSHP_i}(n) \leq av_{PV}(n) \tag{12}$$

where f are power flows with subscripts indicating source and sink, i is GSHP system number, n is time step number, and av_{PV} is the available PV

Table B1
Values used for physical borehole parameters.

Parameter	Value
Borehole distance	7.5 m
Borehole buried depth	4 m
Borehole radius	0.075 m
Inner u-tube radius	0.015 m
Outer u-tube radius	0.020 m
Ground thermal conductivity	2.0 W/(m K)
Grout thermal conductivity	1.0 W/(m K)
Fluid to outer pipe wall thermal resistance	0.1 (K m)/W
Mass flow rate per borehole	0.25 kg/s
Specific heat capacity of fluid	4 000 J/(kg K)
Soil thermal diffusivity	1.0e-6 m^2/s

power.

Selling excess PV to the grid is expressed in the optimization constraint for each time step given in Eq. (13)

$$f_{PV\rightarrow util}(n) \leq max(0, av_{PV}(n) - l_{hw}(n) - l_{el}(n)) \tag{13}$$

where $f_{PV\rightarrow util}$ is the power flow from PV system to utility, av_{PV} is the available PV power, l_{hw} and l_{el} are hot water and electric load demands, and n is time step number.

Self-consumption SC and self-sufficiency SS as defined by Luthander, Widen, Nilsson and Palm [25] are given in Eqs. (14) and (15).

$$SC = \frac{\sum_n f_{PV\rightarrow el}(n) + \eta_{bc}\eta_{bd} f_{PV\rightarrow b}(n) + \sum_i f_{PV\rightarrow GSHP_i}(n)}{\sum_n av_{PV}(n)} \tag{14}$$

$$SS = \frac{\sum_n \left(f_{PV\rightarrow el}(n) + \eta_{bc}\eta_{bd} f_{PV\rightarrow b}(n) + \sum_i f_{PV\rightarrow GSHP_i}(n)\right)}{\sum_n (l_{hw}(n) + l_{el}(n))} \tag{15}$$

Note that PV energy sold to the grid is included in neither nominator, while the total availability is found in the denominator for self-consumption, independent of any curtailment.

GSHP system

The optimization's selection of zero or one GSHP system follows the method of Bordin and Mo [23]. The corresponding optimization constraints are given in Eqs. (16)–(19)

$$\sum_i \mathrm{ex}_i \leq 1 \tag{16}$$

$$M \cdot \mathrm{ex}_i \geq f_{GSHP_i\rightarrow hw}(n) \tag{17}$$

$$M \cdot \mathrm{ex}_i \geq f_{PV\rightarrow GSHP_i}(n) \tag{18}$$

$$M \cdot \mathrm{ex}_i \geq f_{util\rightarrow GSHP_i}(n) \tag{19}$$

where ex_i is 1 if GSHP system number i exists or otherwise 0, M is a big number, and f are power flows with subscripts indicating source and sink. The big number ensures that any flow to and from GSHP system is allowed if ex_i is 1, otherwise no flow if ex_i is 0.

The BHE can either be charged directly, with COP of 1, or by use of an additional air-to-liquid heat pump, which gives a higher COP. According to Norsk Varmepumpeforening [29], a typical air-to-water heat pump has a COP of 2.5–3.5, and ENOVA [52] use 2.7 in their calculations, which is also the default value used in the present work. At the Skarpnes case, presently, there is no option for energy storage in the BHE apart from a heat exchanger between the brine and inlet air which is said to be able to cool the air only slightly [33].

The coefficient of performance COP for the GSHP is defined as shown in Eq. (20)

$$\mathrm{COP} = \frac{Q_{\text{useful heat}}}{Q_{\text{electric}}} \tag{20}$$

where $Q_{\text{useful heat}}$ is the useful heat supplied by the GSHP to the building, while Q_{electric} is the electric energy used to run the GSHP.

The COP is limited by the ideal Carnot cycle value COP_C as given in Eq. (21)

$$\mathrm{COP}_C = \frac{T_h}{T_h - T_{f,out}} \tag{21}$$

where T_h is the high temperature used to heat the building and $T_{f,out}$ is the lower temperature of the liquid entering the heat pump from the BHE. Eq. (21) is further modified by the system efficiency η_{syst} to get an estimate of the actual, effective coefficient of performance as given by Eq. (22).

$$\mathrm{COP} = \eta_{\text{syst}} \cdot \mathrm{COP}_C = \eta_{\text{syst}} \cdot \frac{T_h}{T_h - T_{f,out}} \tag{22}$$

The value of $T_{f,out}$, required to calculate the GSHP COP at any given time, is obtained from the borehole temperature. The borehole temperature is calculated using the model of Cimmino [26]. Temperature response functions, known as g-functions, are a computationally efficient method for simulating BHEs, used with GSHP systems. The g-function g_{func} for a borehole gives the relation between the heat extraction rate Q' in the BHE field and the average temperature variation at the borehole walls T_b as shown in Eq. (23)

$$T_b = T_g - g_{\text{func}} \frac{Q^{`}}{2\pi k_s} \tag{23}$$

where T_g is the undisturbed ground temperature and k_s is the thermal conductivity of the rock.

The present model uses the assumption of uniform borehole wall temperature to determine the g-function for a given BHE field geometry for a time period of 2 years. Subsequently, fluid and ground temperatures are computed for each simulation timestep using the Claesson-Javed algorithm, which consists of the following steps:

1. Aggregate loads
2. Set new heat extraction rate
3. Update the borehole wall temperature
4. Update the fluid temperatures

The borehole wall temperature T_b is updated from Eq. (23), while the heat extraction rate is set according to Eq. (24)

$$Q' = \frac{f_{GSHP_i\rightarrow hw}(n) - f_{PV\rightarrow GSHP_i}(n) - f_{util\rightarrow GSHP_i}(n)}{L} \tag{24}$$

where f is the power flowing to and from the GSHP system with subscripts indicating sources and sinks, i is GSHP system number, n is the time step number, and L is the total length of all boreholes. Eq. (24) shows how the borehole only sees the net extraction rate Q', independent of what combination of energy outtake and energy input caused it.

Eq. (24) assumes that the BHE is always able to store the injected heat, and that the desired heat can always be extracted. An upper limit for the injected and extracted heat is therefore required, and based on typical values from Traaen [28], a value of 35 W/m is used in the present work. This is expressed by the optimization constraints given in Eqs. (25) and (26)

$$f_{GSHP_i\rightarrow hw}(n) \le av_{GSHP_i} \tag{25}$$

$$f_{util\rightarrow GSHP_i}(n) + f_{PV\rightarrow GSHP_i}(n) \le av_{GSHP_i} \tag{26}$$

where f is the power flowing to and from the GSHP system with subscripts indicating sources and sinks, and $av_{GSHP_i}(n)$ is the available power to or from this GSHP system.

During optimization, a simplified version of the above algorithm is used to update the borehole wall temperature T_b, while the temperature difference between T_b and $T_{f,out}$ is assumed to be fixed in K, as shown in Eq. (27).

$$\widehat{T}_{f,out} = T_b - \Delta T_{b-f} \tag{27}$$

This approximation is done to keep all constraints linear and to keep the computational time acceptable.

Once the optimization is run, the full algorithm is used to find the resulting temperatures, and if the difference in the average $T_{f,out}$ during BHE discharge from the approximate method is more than 0.1 K, the optimization is rerun with an updated estimate for the temperature difference ΔT_{b-f}.

Too low ground temperatures will reduce the GSHP performance, as seen in Eq. (22) for COP. To ensure that even several years of use will not lead to too low BHE temperatures, i.e. the BHE is regenerated, the temperature difference between the start and end of a simulation is limited as shown in Eq. (28).

$$T_b(0) - T_b(N) \le \Delta T_{max} \tag{28}$$

The default value for ΔT_{max} is 0.1 K. This limitation is only effective when a whole year is simulated, in practice if the simulated time span is between 364 and 367 days.

To avoid transients of too low temperatures in the ground, the borehole wall temperature is constrained to never go below 273 K for all time steps n as shown in Eq. (29).

$$T_b(n) \ge 273K \tag{29}$$

The use of the GSHP system to cover hot water requirements can be described as shown in Eq. (30)

$$\sum_i \left(f_{GSHP_i\rightarrow hw}(n) \cdot \frac{\text{COP}_i(n)}{\text{COP}_i(n) - 1} \right) \le l_{hw}(n) \tag{30}$$

where the sum is over all GSHP system configurations, $f_{GSHP_i\rightarrow hw}(n)$ is the power flowing from GSHP system i to hot water at time step n, $\text{COP}_i(n)$ is the COP for GSHP in GSHP system number i at time step n, and $l_{hw}(n)$ is the hot water load at time step n. To keep all constrains linear, Eq. (30) was reformulated to Eq. (31), which applies to all timesteps n, resulting in N constraints where N is the total number of time steps.

$$\sum_i \left(f_{GSHP_i \rightarrow hw}(n) \cdot \eta_{syst} T_h\right) \leq l_{hw}(n)\left(\left(\eta_{syst} - 1\right) T_h + T_{f,out}(n)\right) \tag{31}$$

In the present study, the default BHE parameters from the software package pygfunction [26] have been used. These are given in Table B1.

Utility

The utility availability was set to 63 A × 230 V, since this is the upper limit set for an ordinary single-family house by Agder Energi Nett, who supplies the utility grid in Agder county on the south coast of Norway. This is expressed for each time step as the optimization constraint given in Eq. (32), where f are power flows with subscripts indicating source and sink, av_{util} is the utility availability, n is time step number, and i is GSHP system number.

$$f_{util \rightarrow el}(n) + f_{util \rightarrow hw}(n) + \sum_i f_{util \rightarrow GSHP_i}(n) \leq av_{util} \tag{32}$$

Appendix C. Case-study cost details

GSHP system

GSHP system costs were taken from Traaen [28] and Norsk Varmepumpeforening [29]. A summary of the costs is given in Table C1, where the annual investment and installation cost is determined with 5% interest rate over 20 years for the liquid-to-liquid heat pump [38], 15 years for the air-to-liquid heat pump [52], and 100 years for the boreholes. Governmental support [53] is included. Rated power for the heat pumps is set to three different values, 2, 4.7, and 15 kW, to show a relevant price range. In the simulations, 4.7 kW rated power is used, as installed at Skarpnes.

Utility

In Norway, the utility cost for private consumers consists of grid tariff, energy cost, and public taxes. In this study, grid tariff and energy costs are taken from the local companies Agder Energi Nett [54] and LOS [55]. These companies include public taxes and offer prosumer tariffs allowing the customer to sell excess PV electricity back to the grid. Spot prices are taken from Nordpool [56]. Typical total prices are in the range of 0.05–0.1 USD per kWh plus USD 500 per year, while the selling of excess PV electricity can reduce the bill by up to USD 520. Also note that there may be a limit for annual sales of PV electricity to the grid.

For industrial customers and for very large private houses Agder Energi Nett offers a capacity tariff using the maximum peak per month [57], the approach which is implemented in the present work. The price value is taken from Sæle and Bremdal [58], who considered various grid tariffs for households with PV systems installed.

Table C1
Fixed and variable costs for the various components of the case study's possible GSHP systems.

Element	Investment and installation cost per house [USD]	Investment and installation annual cost [USD]	Variable costs [USD/kWh]
One 100 m borehole per house	4120	210	0
Two 100 m boreholes for 5 houses	2250	110	0
Two 200 m boreholes for 5 houses	3250	160	0
Liquid-to-liquid heat pump (2/4.7/15 kW)	1910/5840/20820	160/490/1750	0.0014
Air-to-liquid heat pump (2/4.7/15 kW)	3130/7360/23500	310/730/2320	0

Appendix D. Case-study site and environmental details

Central details on the case-study site and environment are given in Table D1. These parameters are not used directly in the optimization, but they are useful to better understand the case and for comparing this case to other cases.

Table D1
Case-study site and environmental details [33].

Parameter	Value	Source
Building details		
Building completed	2014/2015	[31]
Heated floor area	154 m^2	[33]
Number of floors	2	[33]
Number of bedrooms	4	[31]
Number of occupants	The case is from one of five houses. Each of the five houses is occupied by one family, consisting of two adults with none, one, or two children	[59]
U-values: External walls/roof/floor on ground/ windows and doors	0.12/0.08/0.09/0.80 W/m^2K	[33]
Normalized thermal bridge value	0.03 W/m^2K	[31]
Air tightness, air changes per hour (at 50 Pa)	As built-values: 0.4–0.51	[31]
Energy system details		
Total installed PV capacity	7.36 kW_p	[31]
PV inverter	Type: SMA Sunny Tripower 7000TL-20 (3-phase), size: 7 kW, max efficiency: 98%, max DC power: 7 175 W, max AC power (230 V, 50 Hz): 7 000 W	[33]
Heat pump type	IVT PremiumLine HQ Model C4,5 (liquid/water heat pump)	[33]
Electric element for DHW heating	9 kW	[33]
DHW hot water tank size	180 l	[33]
Accumulator tank for floor/room heating size	40 l	[33]
Balanced ventilation system	Type: Systemair VR 300 ECV/B, efficiency: 86%, size: 1.0 kW	[33]
Fan convector	Type: Aeros, Lyngson SL 400 - SL600 - SL800, heating 4.0–5.5–7.0 kW, cooling 1.8–2.7–3.3 kW	[33]
Circulation pump	Grundfos 25–40 130 Alpha 2l, size 25–45 W	[33]
Climate details		
Geographic position	58.43°N, 8.72°E	[31]
Average outdoor temperature	8.3 °C	[47]
Monthly solar irradiation	190–6400 Wh/m^2 per day	[35]
Annual average solar irradiation	1100 kWh/m^2	[60]

Appendix E. Case-study data details

Electric load

The time period May 1, 2015 to April 30, 2016 has high-quality data about electrical loads for the chosen house, except for a few larger periods of missing data and some data spikes with value 0. Obviously erroneous 0-values and small lengths of missed data have been removed and bridged via linear interpolation. Larger lengths of missed data, as those in the month of August, have been replaced by copying values from future times. Future time is chosen rather than past since July is the vacation month in Norway, and therefore not representative for demand behavior for August.

The ABB A41/42 power meters used here have 1% accuracy [33]. The interpolation and replacement of missing data can be estimated to add another 20% uncertainty to these particular data points. Note that the data logged is the total energy consumption since the start of logging, which was prior to the simulation year used in the present work. After a period of missing data, this value had increased about as much as could be expected. This indicates that the problem was in the data storage, rather than in the measurement itself. The added uncertainty for the missing data points does therefore not apply to the total energy requirement for the whole year. Neither does it affect the distribution between the months of the year.

Hot water load

Continuous data on this total hot water load is available from mid-April 2015 to April 2016 except for a few larger ranges of missing data. These data gaps have been interpolated and replaced in the same manner as for electric loads.

The Kamstrup Multical 402 flow meters used [33] have about 2% accuracy, higher for flow rates below 0.06 m^3/s [61]. As for the electric loads, the data logged is the total energy consumption since the start of logging. Consequently, all handling of missing data points will only influence the load distribution within the missing period, which is always less than 1 month. The total energy consumption for the whole year is not influenced, and neither is the distribution between the months of the year.

PV energy generated

The PV energy data from Skarpnes has long periods of missing data and sensors not working. However, solar irradiation, global horizontal irradiation (GHI), has been monitored over long periods. For some days in March–April 2017, both energy from the solar cell inverter and solar irradiation data are available. Thus, a regression analysis was performed to estimate the available PV energy from the solar irradiation data, resulting in a regression coefficient of 6.63 $Wh/(Wh/m^2)$. Even the solar irradiation data had missing values, which have been replaced by data from the same month of the past/next year or as a minute-by-minute average of the month before and after the missing month.

The solar irradiation was measured by a Kipp & Zonen CMP11 pyranometer with directional response error $<10\ W/m^2$ up to 80° zenith angle and temperature sensitivity <1% [33]. The registered energy generation for the days used in the regression were between 4000 and 41000 Wh. The R^2 value for the regression was 0.999, the root mean square error was 700 Wh, and the standard error of the coefficient was 0.05 $Wh/(Wh/m^2)$. The resulting total uncertainty of the daily PV energy generation is dominated by the regression uncertainty, giving 200 Wh for the typical daily PV energy generation of 27000 Wh, i.e. less than 1%.

The measured solar irradiation for the days used for regression were between 560 and 6300 Wh/m^2 per day. According to PVGIS [35], the monthly sum of solar irradiation for the simulated year was between 190 and 6 400 Wh/m^2 per day. Since GHI is used as the measure of solar irradiation, the variation in solar angles is already taken into account. Thus, the solar irradiation data used for the regression is representative for the whole year.

According to ZERO [60], the annual average solar irradiation in northern Norway is 700 kWh/m^2, and about 1 100 kWh/m^2 in southern Norway. According to the same source, a sunny summer day in southern Norway may give as much as 8500Wh/m^2, while a cloudy winter day in the same region may give 20 Wh/m^2.

GSHP system

At Skarpnes, the undisturbed ground temperature is 8.5 °C, and the water is heated to 55 °C [33]. Norway is located on the Fennoscandian Shield, where the lithosphere is cool and thick, characterized by a low heat flow density [43]. The ground temperature at Skarpnes is typical for the Norwegian ground, where the temperature 150–200 m below ground is usually 6–8 °C [62].

According to the Skarpnes project report [33], the liquid-to-liquid heat pump COP is 4.2, corresponding to a system efficiency of 0.60.

References

[1] IEA. Buildings – A source of enormous untapped efficiency potential. IEA; 2021. https://www.iea.org/topics/buildings (accessed May 27, 2021).

[2] Global Warming of 1.5°C. An IPCC Special Report on the impacts of global warming of 1.5°C above pre-industrial levels and related global greenhouse gas emission pathways, in the context of strengthening the global response to the threat of climate change, sustainable development, and efforts to eradicate poverty. IPCC; 2018.

[3] European Commission. Commission presents Renewable Energy Directive revision. European Commission; 2021. https://ec.europa.eu/info/news/commission-presents-renewable-energy-directive-revision-2021-jul-14_en (accessed August 22, 2021).

[4] European Commission. Energy performance of buildings directive. European Commission; 2019. https://ec.europa.eu/energy/topics/energy-efficiency/energy-efficient-buildings/energy-performance-buildings-directive_en (accessed August 22, 2021).

[5] IEA – International Energy Agency Energy. Energy policies of IEA Countries: Norway 2017 Review. IEA; 2017. https://www.iea.org/reports/energy-policies-of-iea-countries-norway-2017-review (accessed May 6, 2021).

[6] ENOVA. Tenker du å oppgradere boligen din? [Do you plan to upgrade your home?]. Enova; 2021. https://www.enova.no/privat/ (accessed August 22, 2021).

[7] Bundesamt für Wirtschaft und Ausfuhrkontrolle. BAFA - Fördervoraussetzungen [BAFA - Eligibility requirements]; 2021. https://www.bafa.de/DE/Energie/Heizen_mit_Erneuerbaren_Energien/Foerdervoraussetzungen/foerdervoraussetzungen_node.html (accessed August 22, 2021).

[8] Enkhardt S. Germany introduces new renewable energy law. Pv Mag Int 2020.

[9] Ofgem. Smart Export Guarantee (SEG). Ofgem; 2020. https://www.ofgem.gov.uk/environmental-and-social-schemes/smart-export-guarantee-seg (accessed August 22, 2021).

[10] Sommerfeldt N , Madani H Review of solar PV/thermal plus ground source heat pump systems for European multi-family houses . Eurosun, Palma de Mallorce, Spain 2016 . doi: 10.18086/eurosun.2016.08.152016 .

[11] Alonso MJ, Ramstad RK, Holmberg H, Walnum HT, Midttømme K, Andersen G. Fjell 2020 high temperature borehole energy storage - system control for various operation modes, World Geothermal Congress 2020, Reykjavik, Iceland; 2020.

[12] Shakerin M, Eikeskog V, Li Y, Thorgeir HT, Nord N. Sizing and performance analyses of a combined heating and cooling system with the integration of short- and long-term storages. E3S Web Conf 2021;246:07004. Doi: 10.1051/e3sconf/202124607004.

[13] Korkas CD, Baldi S, Michailidis I, Kosmatopoulos EB. Occupancy-based demand response and thermal comfort optimization in microgrids with renewable energy sources and energy storage. Appl Energy 2016;163:93–104. https://doi.org/10.1016/j.apenergy.2015.10.140.

[14] Alimohammadisagvand B, Jokisalo J, Kilpeläinen S, Ali M, Sirén K. Cost-optimal thermal energy storage system for a residential building with heat pump heating and demand response control. Appl Energy 2016;174:275–87. https://doi.org/10.1016/j.apenergy.2016.04.013.

[15] Williams CJC, Binder JO, Kelm T. Demand side management through heat pumps, thermal storage and battery storage to increase local self-consumption and grid compatibility of PV systems. In: 2012 3rd IEEE PES Innovative Smart Grid Technologies Europe (ISGT Europe); 2012. p. 1–6. https://doi.org/10.1109/ISGTEurope.2012.6465874.

[16] Salpakari J, Lund P. Optimal and rule-based control strategies for energy flexibility in buildings with PV. Appl Energy 2016;161:425–36. https://doi.org/10.1016/j.apenergy.2015.10.036.

[17] Litjens GBMA, Worrell E, van Sark WGJHM. Lowering greenhouse gas emissions in the built environment by combining ground source heat pumps, photovoltaics and battery storage. Energy Build 2018;180:51–71. https://doi.org/10.1016/j.enbuild.2018.09.026.

[18] Kavian S, Aghanajafi C, Jafari Mosleh H, Nazari A, Nazari A. Exergy, economic and environmental evaluation of an optimized hybrid photovoltaic-geothermal heat pump system. Appl Energy 2020;276. https://doi.org/10.1016/j.apenergy.2020.115469.

[19] Beck T, Kondziella H, Huard G, Bruckner T. Optimal operation, configuration and sizing of generation and storage technologies for residential heat pump systems in the spotlight of self-consumption of photovoltaic electricity. Appl Energy 2017;188:604–19. https://doi.org/10.1016/j.apenergy.2016.12.041.

[20] Erdinc O, Paterakis NG, Pappi IN, Bakirtzis AG, Catalão JPS. A new perspective for sizing of distributed generation and energy storage for smart households under demand response. Appl Energy 2015;143:26–37. https://doi.org/10.1016/j.apenergy.2015.01.025.

[21] Sim M, Suh D, Otto M-O. Multi-Objective Particle Swarm Optimization-Based Decision Support Model for Integrating Renewable Energy Systems in a Korean Campus Building. Sustainability 2021;13:8660. https://doi.org/10.3390/su13158660.

[22] Hauer A, Teuffel A. Integration of Energy Storage into Energy Systems. Handbook of Clean Energy Systems. Am Cancer Society 2015:1–14. https://doi.org/10.1002/9781118991978.hces215.

[23] Bordin C, Mo O. Including power management strategies and load profiles in the mathematical optimization of energy storage sizing for fuel consumption reduction in maritime vessels. J Storage Mater 2019;23:425–41. https://doi.org/10.1016/j.est.2019.03.021.

[24] Kenton W. How Equivalent Annual Cost Helps with Capital Budget Decisions. Investopedia; 2020. https://www.investopedia.com/terms/e/eac.asp (accessed February 23, 2021).

[25] Luthander R, Widén J, Nilsson D, Palm J. Photovoltaic self-consumption in buildings: A review. Appl Energy 2015;142:80–94. https://doi.org/10.1016/j.apenergy.2014.12.028.

[26] Cimmino M. pygfunction: an open-source toolbox for the evaluation of thermal response factors for geothermal borehole fields 2018:10.

[27] Python-MIP; 2020. https://www.python-mip.com/ (accessed March 16, 2021).

[28] Traaen KB. Bergvarmepumper - lokale eller kollektive energibrønner? [Ground Source Heat Pumps - local or central energy wells?]. Master thesis. NMBU; 2018.

[29] Varmepumpeforeningen. Alt om luft-til-vann-varmepumper – Varmepumpeforeningen [All about air-to-water-heat pumps – The heat pump association]. Varmepumpeinfo.no; 2020. https://www.varmepumpeinfo.no/varmepumpetyper/luft-til-vann-varmepumpe (accessed February 12, 2021).

[30] Mook V. DSO tariffs in Norway; 2016.

[31] Sørensen ÅL, Imenes AG, Grynning S. Dokka TH Energy measurements at Skarpnes zero energy homes in Southern Norway: Do the loads match up with the on-site energy production? Energy Procedia 2017:567–73. https://doi.org/10.1016/j.egypro.2017.09.743.

[32] Thyholt M, Dokka TH, Rasmussen R. The Skarpnes residential development - a zero energy pilot project, Trondheim, Norway; 2012.

[33] Imenes AG. NFR EnergiX project 226139 Electricity Usage in Smart Village Skarpnes - Report 1 Instrumentation and Data Collection. Grimstad, Norway: Teknova AS; 2017.

[34] Multiconsult, Asplan Viak. Solcellesystemer og sol i systemet [Solar cell systems and sun in the system]; 2018.

[35] JRC Photovoltaic Geographical Information System (PVGIS) - European Commission; 2019. https://re.jrc.ec.europa.eu/pvg_tools/en/tools.html#PVP (accessed August 28, 2021).

[36] Brødrene Dahls Varmebok, Kapittel 1 Energi- og effektberegning [The Dahl brothers' book of heating, Chapter 1 Calculation of energy and power]. Brødrene Dahl; 2018.

[37] Parra D, Swierczynski M, Stroe D, Norman S, Abdon A, Worlitschek J, et al. An interdisciplinary review of energy storage for communities: Challenges and perspectives. Renew Sustain Energy Rev 2017;79:730–49. https://doi.org/10.1016/j.rser.2017.05.003.

[38] ENOVA. Kjøpsveileder Væske-til-vann-varmepumpe En veileder fra Enova og Miljødirektoratet [Purchasing guide for liquid-to-water heat pumps. A guide from Enova and the Norwegian Environment Agency]; 2016.

[39] Skarphagen H, Banks D, Frengstad BS, Gether H. Design Considerations for Borehole Thermal Energy Storage (BTES): A Review with Emphasis on Convective Heat Transfer. Geofluids 2019;2019. https://doi.org/10.1155/2019/4961781.

[40] HEATSTORE. Heatstore - High Temperature Thermal Energy Underground Storage; 2021. https://www.heatstore.eu/ (accessed May 9, 2021).

[41] Energy consumption in households; 2021. https://ec.europa.eu/eurostat/statistics-explained/index.php?title=Energy_consumption_in_households (accessed August 30, 2021).

[42] Garabetian Thomas. Geothermal energy in Europe; Geothermal Energy Workshop . GCE NOCE and CGER ; 2020.

[43] Midttømme K , Justo Alonso M , Krafft C , Kvalsvik K , Ramstad R , Stene J Geothermal Energy Use in Norway, Country Update for 2015-2019 . World Geothermal Congress 2020, Reykjavik, Iceland 2020.

[44] Casasso A, Sethi R. Assessment and Minimization of Potential Environmental Impacts of Ground Source Heat Pump (GSHP) Systems. Water 2019;11:1573. https://doi.org/10.3390/w11081573.

[45] Geothermal energy - Environmental effects and economic costs. Encyclopedia Britannica; 2014. https://www.britannica.com/science/geothermal-energy/Environmental-effects-and-economic-costs (accessed August 31, 2021).

[46] Observations and weather statistics. Norwegian Centre for Climate Services; 2021. https://seklima.met.no/observations/ (accessed March 16, 2021).

[47] Weather statistics for Arendal. Yr; 2021. https://www.yr.no/en/statistics/table/1-7396/Norway/Agder/Arendal/Arendal?q=last-13-months (accessed May 18, 2021).

[48] Spitler J, Cook J, Liu X (ORCID:000000028457249X). Recent Experiences Calculating g-functions for Use in Simulation of Ground Heat Exchangers. Oak Ridge National Lab. (ORNL), Oak Ridge, TN (United States); 2020.

[49] COIN-OR: Computational Infrastructure for Operations Research. COIN-OR: Computational Infrastructure for Operations Research; 2016. https://www.coin-or.org/ (accessed August 28, 2021).

[50] Litjens G, Worrell E, van Sark W. Economic benefits of combining self-consumption enhancement with frequency restoration reserves provision by photovoltaic-battery systems. Appl Energy 2018;223:172–87. Doi: 10.1016/j.apenergy.2018.04.018.

[51] Tesla Powerwall Review 2021. Clean Energy Reviews; 2021. https://www.cleanenergyreviews.info/blog/tesla-powerwall-2-solar-battery-review (accessed February 20, 2021).

[52] ENOVA. Kjøpsveileder Luft-til-vann-varmepumpe En veileder fra Enova og Miljødirektoratet [Purchasing guide for air-to-water heat pumps. A guide from Enova and the Norwegian Environment Agency]; 2016.

[53] Varmepumper - Spar energi og penger [Heat pumps - Save energy and money]. Enova; 2017. https://www.enova.no/privat/alle-energitiltak/varmepumper/ (accessed March 16, 2021).

[54] Agder Energi. Nettleiepriser 2020 Privatkunder [Grid tariffs 2020 Private customers] 2019. Fhfgch*.

[55] LOS solstrøm [LOS solar electricity]. LOS; 2020. https://www.los.no/strom/solstrom/ (accessed December 20, 2020).

[56] Historical Market Data; 2020. https://www.nordpoolgroup.com/historical-market-data/ (accessed December 20, 2020).

[57] Agder Energi. Effektmåling [Power measurement]. Agder Energi; 2019. https://www.aenett.no/kundeforhold/kundebetingelser/kundebetingelser-bedriftskunde/effektmaling/ (accessed March 5, 2021).

[58] Sæle H, Bremdal B. Economic evaluation of the grid tariff for households with solar power installed. CIRED - Open Access Proc J 2017;2017:2707–10. https://doi.org/10.1049/oap-cired.2017.0556.

[59] Moum Anita, Hauge Åshild Lappegard, Thomsen Judith. Casebeskrivelser av fire norske ZEB pilotbygg – byggeprosess og brukerevaluering SINTEF Bokhandel [Case descriptions of five Norwegian ZEB pilot buildings - building process and user evaluation]. SINTEF; 2017.

[60] Arendal kommune. Forslag kommunedelplan KLIMA- OG ENERGI Arendal 2018 [Suggested municipality plan, climate and energy, Arendal 2018]; 2018.

[61] Kamstrup Multical 402 Energy Flow Meters | ABLE. ABLE Instruments & Controls; 2021. https://able.co.uk/product/flow/energy-flow-meters/heating-cooling/multical-402/ (accessed August 28, 2021).

[62] Energy Underfoot. SINTEF; 2010. https://www.sintef.com/en/latest-news/2010/energy-underfoot-/ (accessed August 28, 2021).